Hantavirus Pulmonary Syndrome

Pathogenesis of an Emerging Infectious Disease

Sherif R. Zaki,* Patricia W. Greer,*
Lisa M. Coffield,* Cynthia S. Goldsmith,*
Kurt B. Nolte,† Kathy Foucar,†
Richard M. Feddersen,† Ross E. Zumwalt,†
Gayle L. Miller,* Ali S. Khan,* Pierre E. Rollin,*
Thomas G. Ksiazek,* Stuart T. Nichol,*
Brian W.J. Mahy,* and Clarence J. Peters*

From the Division of Viral and Rickettsial Diseases,
National Center for Infectious Diseases, Centers for Disease
Control and Prevention, Atlanta, Georgia; and Department
of Pathology,† University of New Mexico School of Medicine,
Albuquerque, New Mexico*

A recent outbreak of a severe pulmonary disease in the southwestern United States was etiologically linked to a previously unrecognized hantavirus. The virus has been isolated from its major reservoir, the deer mouse, Peromyscus maniculatus, *and recently named Sin Nombre virus. Clinically, the disease has become known as the hantavirus pulmonary syndrome (HPS). Since May 1993, 44 fatal cases of HPS have been identified through clinicopathological review and immunohistochemical (IHC) testing of tissues from 273 patients who died of an unexplained noncardiogenic pulmonary edema. In 158 cases for which suitable specimens were available, serological testing and/or reverse transcription-polymerase chain reaction (RT-PCR) amplification of extracted RNA was also performed. IHC, serological, and PCR results were concordant for virtually all HPS and non-HPS patients when more than one assay was performed. The prodromal illness of HPS is similar to that of many other viral diseases. Consistent hematological features include thrombocytopenia, hemoconcentration, neutrophilic leukocytosis with a left shift, and reactive lymphocytes. Pulmonary histopathological features were similar in most of the fatal HPS cases (40/44) and consisted of an interstitial pneumonitis with a variable mononuclear cell infiltrate, edema, and focal hyaline membranes. In four cases, however, pulmonary features were significantly different and included diffuse alveolar damage and variable degrees of severe air space disorganization. IHC analysis showed widespread presence of hantaviral antigens in endothelial cells of the microvasculature, particularly in the lung. Hantaviral antigens were also observed within follicular dendritic cells, macrophages, and lymphocytes. Hantaviral inclusions were observed in endothelial cells of lungs by thin-section electron microscopy, and their identity was verified by immunogold labeling. Virus-like particles were seen in pulmonary endothelial cells and macrophages. HPS is a newly recognized, often fatal disease, with a spectrum of microscopic morphological changes, which may be an important cause of severe and fatal illness presenting as adult respiratory distress syndrome. (Am J Pathol 1995, 146:552–579)*

In May 1993, the deaths of several previously healthy individuals from a rapidly progressive illness were reported by health care workers in the southwestern United States.[1] The patients developed an influenza-like illness followed by a rapidly progressive pulmonary edema, respiratory insufficiency, and shock. Results of initial intensive and broad-based laboratory testing of patient specimens for bacterial, viral, and toxicological agents were negative. Patient specimens were forwarded to the Centers for Disease Control and Prevention (CDC) for further studies. Using immunoassays, Ksiazek and co-workers[2] detected cross-reactive antibodies to known hantaviral antigens in the serum of the patients, suggesting a previously unrecognized hantavirus as the cause of the disease. This observation was quickly confirmed by the demonstration of hantaviral antigens and nucleic

acid sequences in autopsy tissues by using immu-nohistochemical (IHC) and polymerase chain reac-tion (PCR) techniques.[3–6] The causative agent was recently isolated at CDC from a deer mouse, *Pero-myscus maniculatus*, the natural reservoir and vector of this zoonotic virus, and has been subsequently named Sin Nombre virus (SNV).[7,8]

Hantaviruses include a group of closely related, trisegmented, negative-sense RNA viruses of the family *Bunyaviridae*.[9–11] Several distinct serotypes of these viruses are distributed throughout the world, each associated with a different primary rodent res-ervoir.[12,13] Hantaviruses are transmitted to humans by direct contact with or inhalation of aerosolized ro-dent excrement. All hantavirus-associated illnesses known prior to the outbreak of HPS share various de-grees of fever and renal involvement, with or without hemorrhagic manifestations, and are referred to col-lectively as hemorrhagic fever with renal syndrome (HFRS).[14] The pronounced pulmonary involvement, which is a hallmark of HPS, has not been a prominent feature of HFRS.[15] Hantaan (HTN) virus causes the most severe and often fatal form of HFRS, formerly known as Korean hemorrhagic fever in Korea and epi-demic hemorrhagic fever in Japan and China. Seoul (SEO) virus, which is distributed worldwide, causes a less severe form of the disease and has been diag-nosed most frequently in Asia. Puumala (PUU) virus is the agent responsible for the mildest form of HFRS, namely nephropathia epidemica, in Scandinavia and Western Europe. Prospect Hill (PH) virus is indig-enous to the United States, but has not been asso-ciated with human disease.

In this report we describe 1) the laboratory inves-tigation that led to the identification of the virus in au-topsy tissues, 2) the clinicopathological findings as well as the IHC distribution of SNV antigens in tissues of HPS patients, and 3) some of the unusual aspects of the pathology and pathophysiology of this viral in-fection.

Materials and Methods

Patient Tissues

Tissues from 273 patients with unexplained noncar-diogenic pulmonary edema were submitted to CDC for pathological and immunopathological evaluation of hantavirus infection. Tissues were received either fixed in formalin or embedded in paraffin. In a limited number of cases, frozen tissues and glutaraldehyde-fixed specimens were also available for immunohis-tological and electron microscopic (EM) studies. Se-rum, plasma, and/or frozen tissues were available for microbiological, serological, and PCR testing in 158 cases. In all cases, routine hematoxylin and eosin (H&E) sections and autopsy reports were reviewed. Gomori methenamine silver, Brown and Brenn, acid fast, periodic acid Schiff, and Giemsa stains were per-formed and evaluated for the first 15 cases and se-lected cases thereafter.

Cell Lines

Controls for light-microscopic IHC studies were gen-erated from formalin-fixed and paraffin-embedded pellets of minced normal human tissues mixed with either noninfected Vero E6 (Vero clone CRL 1586, American Type Culture Collection (Rockville, MD)) cells or Vero cells infected with PUU, PH, SEO, HTN, and SN viral strains. The noninfected and various in-fected Vero cells were grown and maintained in Ea-gle's minimum essential medium (EMEM) supple-mented with 5% heat-inactivated fetal bovine serum as previously described.[8]

Antibodies

The antibodies used in this study are listed in Table 1. Tissues from all cases were examined by IHC using the GB04-BF07 monoclonal antibody (MAb).[16] Tis-sues from HPS-confirmed cases were also immunos-tained using *P. maniculatus* and rabbit polyclonal im-mune sera. Paraffin-embedded tissues and γ-irradiated (5×10^6 rads) frozen tissues from some confirmed HPS cases were examined by using non-hantaviral antibodies listed in Table 1.

Immunohistochemistry

Hantaviral Assays

Four-μ sections of tissues placed on Fisher Plus slides (Fisher Scientific, Pittsburgh, PA) were depar-affinized and rehydrated in graded alcohol incuba-tions. For IHC analysis using hantaviral MAbs; tissue sections were then digested in 0.1 mg/ml Proteinase K (Boehringer-Mannheim Corporation, Indianapolis, IN) in 0.6 M Tris (pH 7.5)/0.1% $CaCl_2$ and blocked with normal rabbit serum. The MAbs were then applied to tissue sections and allowed to incubate for 90 min-utes. Optimal dilutions of primary antibody and di-gestion conditions were determined by a series of previous titration experiments. This was followed by sequential application of rabbit anti-mouse link anti-body, alkaline phosphatase anti-alkaline phos-phatase (APAAP) complex, and naphthol/fast red

Table 1. *Antibodies Used in this Study*

Antibody designation	Antigen/target	Source	Working dilution	IHC procedure
Hantaviral				
GB04-BF07	NP/PUU	CDC[16]	1:300	*
DA03-AA12	NP/PUU	CDC[16]	1:300	*
AA02-BE06	NP/PUU	CDC[16]	1:300	*
DC03-AB07	NP/SEO	CDC[16]	1:300	*
KA06-BA10	NP/SEO	CDC[16]	1:300	*
FB03-BC02	G1/SEO	CDC[16]	1:300	*
HC02-BD05	G2/HTN	CDC[16]	1:300	*
EC02-BD01	G1/HTN	CDC[16]	1:300	*
Convalescent HPS sera	SNV	CDC	1:100	†
PM sera	SNV	CDC	1:50	‡
Rabbit polyclonal	SNV	CDC	1:2000	§
Non-hantaviral				
JC/70A	CD31/endothelial cell	Dako	1:25	‖
Rabbit sera	Factor VIII/endothelial cell	Dako	1:200	‖
L26	CD20/B cells	Dako	1:50	*
Rabbit sera	CD3/T cells	Dako	1:50	§, ‖
KP1	CD68/macrophages & granulocytes	Dako	1:75	*, ‖
DF-T1	CD43/T cells & myeloid	Dako	1:25	§
FDC1-p	Follicular dendritic cells	¶88	1:40	§
Ki-M1P	Monocyte/macrophages	¶89	1:100	§, ‖
MT310	CD4/T helper-inducer	Dako	1:15	*
DK25	CD8/T suppressor-cytotoxic T cells	Dako	1:100	*

CDC = Centers for Disease Control and Prevention; G1 = Glycoprotein 1; G2 = Glycoprotein 2; HPS = Hantavirus pulmonary syndrome; NP = Nucleoprotein; PM = *Peromyscus maniculatus;* PUU = Puumala virus; SEO = Seoul virus.
*Alkaline phosphatase anti-alkaline phosphatase method (APAAP).
†Avidin-biotin complex method (ABC).
‡Anti-*Peromyscus* immunoalkaline phosphatase conjugate.
§Streptavidin alkaline phosphatase method (SAAP).
‖Double-labeling method.
¶Gift from Dr. M.R. Parwaresch, Kiel, Germany.

substrate (Dako Corporation, Carpinteria, CA). Sections were then counterstained in Meyer's hematoxylin (Fisher Scientific, Pittsburgh, PA) and mounted with aqueous mounting medium (Signet Laboratories, Dedham, MA).

Immobilized polyclonal *P. maniculatus* antibody was localized by using an alkaline phosphatase goat anti-*Peromyscus* conjugate (Kirkegaard and Perry Laboratories Inc., Gaithersburg, MD), followed by naphthol/fast red incubation.

IHC assays with rabbit sera were performed using the streptavidin alkaline phosphatase (SAAP) method (Dako Corporation). Briefly, after being blocked in normal swine serum, the tissues were incubated with the primary antibody for 1 hour. Biotinylated swine anti-rabbit antibodies were then applied followed by an avidin enzyme complex. Alkaline phosphatase activity was detected as described above.

IHC assays with convalescent-phase sera from HPS patients were performed by the avidin-biotin immunoalkaline phosphatase method, using biotinylated anti-human IgG or IgM (Vector Laboratories, Burlingame, CA) and an avidin-biotin enzyme complex (ABC) method. The specificity of hantaviral histochemical staining was confirmed in all instances by replacing first antibodies with phosphate-buffered sa-

line (PBS) or indifferent antibodies (isotype-identical murine antibodies and nonimmune sera). As an additional negative control, the GB04-BF07 antibody absorbed with excess hantaviral antigen (SNV cell culture lysate) was also used. Control tissues included infected and noninfected cell lines as well as nonhantavirus autopsy tissues.

Phenotypical Analysis of Cell Lineages (Non-Hantaviral Assays)

A series of MAbs and polyclonal sera were used to identify endothelial cells and the nature of the mononuclear cell infiltrates in paraffin-embedded tissues of lung, liver, and spleen using the APAAP and SAAP methods as described above (Table 1). The source of these antibodies, the dilution, and the IHC procedure used are described in Table 2. For analysis of CD4 and CD8, the frozen sections were air dried, fixed in acetone, dried again, and immunostained by using the APAAP method.

Double-Labeling Techniques

Double IHC labeling, combining immunoperoxidase and immunoalkaline phosphatase, was performed for the following couples of antigens (targets):

Table 2.   *Reactivity of Anti-hantaviral Antibodies with Control Cell Lines and Human Tissues*

| | Monoclonal antibodies | | | | | | | | Polyclonal antibodies | | | |
| | PUUMALA | | | HANTAAN | | SEOUL | | | Human convales-cent Sera | P. *maniculatus* Sin Nombre | Rabbit Sin Nombre | Normal* |
Tissue	GB04-BF07	DA03-AA12	AA02-BE06	EC02-BD01	HC02-BD05	KA06-BA10	DC03-AB07	FB03-BC02				
SEO	4+	–	–	4+	4+	2+	4+	2+	2+	–	1+	–
PUU	4+	2+	–	–	–	–	–	–	3+	3+ focal	3+	–
HTN	2+	–	–	4+	4+	–	–	–	1+	–	2+	–
PH	4+	–	–	–	–	–	–	–	3+	3+	4+	–
SN	4+	–	–	–	–	–	–	–	4+	4+	4+	–
Vero	–	–	–	–	–	–	–	–	–	–	–	–
HPS	4+	–	–	–	–	–	–	–	+/–†	4+	4+	–
Non-HPS	–	–	–	–	–	–	–	–	–†	–	–	–

*Normal rabbit, mouse, and human sera controls.
†High background staining.
HTN = Hantaan; HPS = Hantavirus pulmonary syndrome autopsy tissue; Non-HPS = Non-hantavirus pulmonary syndrome autopsy tissue; PH = Prospect Hill; PUU = Puumala; SEO = Seoul; SN = Sin Nombre.
Note: The intensity of staining is expressed on a scale of – to 4+.

CD31/SNV, FVIII/SNV, CD3/CD68, and CD3/Ki-M1P. Primary antibodies were simultaneously incubated on the same section. This was followed by incubation with the respective species-specific link anti-immunoglobulin and serial application of mouse APAAP and rabbit peroxidase antiperoxidase (PAP) reagents. Mouse primary antibodies were then localized by determining the alkaline phosphatase activity, using naphthol/fast red substrate to obtain red deposits. Rabbit primary antibody was localized by incubating the sections in hydrogen peroxide/DAB to detect peroxidase activity in the form of brown deposits.

Ultrastructural IHC

Ultrastructural IHC was performed using a postembedded, indirect immunogold technique. Tissues embedded in LR White resin (London Resin Company, UK) were sectioned and placed on nickel mesh grids. Antibodies used included antisera from infected or uninfected P. maniculatus (1:50 dilution) and GB04-BF07 MAb (1:100 dilution) along with unrelated mouse MAb and nonimmune sera controls. Dilution and rinse buffers consisted of 0.01M PBS, 1% bovine serum albumin (BSA), 0.2% Tween 20, and 0.1% Triton-X. Tissues were incubated either at 4 C overnight or at room temperature for 2 hours with the primary antibody at the appropriate dilution, rinsed, and then incubated for 2 hours with goat anti-mouse serum conjugated with 10-nm gold particles. After being rinsed, sections were stained with 1% osmium and uranyl acetate.

Serology

Serum or plasma was frozen and stored at –70 C after separation of the cellular elements by centrifugation.

IgG and IgM enzyme-linked immunosorbent assays (ELISAs) for SEO and SN viruses are described elsewhere.[17,18]

Briefly, IgG ELISAs were performed by coating polyvinyl chloride microtiter plates overnight at 4 C with either a basic buffer detergent extract of SEO virus-infected Vero cells, further inactivated by 2 × 10^6 rads from a ^{60}Co source or an *Escherichia coli*-expressed SNV nucleocapsid antigen. An uninfected antigen control was run for each serum. IgM antibodies against SN and SEO viruses were detected by capturing IgM from serum with goat anti-human Mu-chain (Tago, Burlingame, CA) adsorbed to the wells of microtiter plates, and then allowing the captured IgM to react with viral antigen (sonicated suspensions of infected or uninfected cells, inactivated with 5 × 10^6 rads from a ^{60}Co source) and measuring bound antigen by the use of hyperimmune rabbit serum and appropriate enzyme conjugate and substrate. A serum dilution was classified as positive if optical density was >0.10 units after adjustment for an appropriate negative antigen. Sera with titers ≥400 obtained when using SEO or SN virus antigens in the IgM test were regarded as diagnostic of acute infection.

## Tissue RNA Extraction and Purification, and Viral RNA Amplification by RT-PCR

RNA extractions and RT-PCR assays were carried out essentially as described previously.[5,19] The RT-PCR assay consisted of a nested pair of reactions, using four primers based on M-segment sequence regions conserved among SN, PH, and PUU viruses. The use of such nested PCR primers provided extra sensitivity and specificity. The DNA resulting from the PCR amplification was subjected to gel electrophoresis and

automated thermocycle sequencing analysis. To avoid generation of infectious aerosols, or cross-contamination of RNA templates and PCR products, the following precautions and controls were employed. Each of the main steps, 1) sample (autopsy tissue, blot clot, or serum) homogenization and RNA extraction and purification, 2) RT-PCR assay, and 3) PCR product electrophoresis and sequence analysis, was performed in different rooms, using biohazard containment hoods in biosafety level 3 facilities for steps 1 and 2. A new pair of disposable gloves was used for each tissue homogenization, aerosol barrier-plugged pipette tips were used, and only one sample tube was open at any given time during all steps. Several water negative controls from the tissue homogenization, first-round RT-PCR, and second-round PCR steps were similarly processed and assayed to check for possible cross-contamination at each stage. Authenticity of all PCR products was verified by nucleotide sequence analysis of the amplified product.

Results

Hantaviral IHC Assays

The serological detection of cross-reactive antibodies to known hantaviral antigens suggested that the unexplained respiratory illness was caused by a previously unknown hantavirus. To confirm this finding and to localize the potentially new virus in human tissues, IHC assays for hantaviral antigens in fixed tissues were developed. A battery of hantavirus-specific MAbs, convalescent-phase human sera from case patients, and polyclonal antibodies that were available early during the outbreak were evaluated by using formalin-fixed, paraffin-embedded, uninfected and hantavirus-infected cell pellets. Figure 1, A and B shows the characteristic finely granular staining of PUU-infected cells with the GB04-BF07 MAb and absence of staining of the adjacent noninfected human control tissue. Several MAbs were found to react specifically with hantaviral antigens in formalin-fixed tissues. Moreover, one of these MAbs (GB04-BF07) was found to cross-react with major hantaviral serotypes
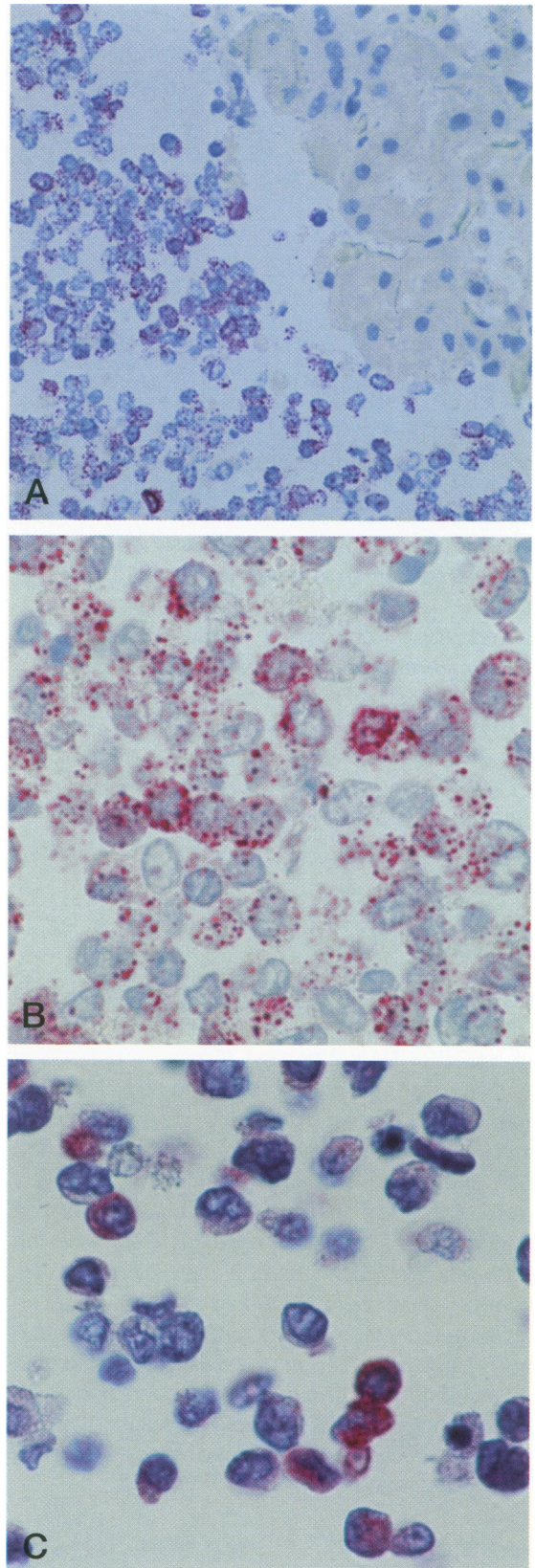
Figure 1. *Immunohistochemical detection of hantaviral antigens in infected cell lines, using GB04-BF07 MAb and convalescent-phase serum.* (A) *Low-power photomicrograph showing immunostaining of PUU virus-infected cells using GB04-BF07 MAb. Note absence of staining of adjacent noninfected human kidney tissue.* (B) *Higher-power magnification of infected cells showing the characteristic cytoplasmic and finely granular deposits of hantaviral antigens.* (C) *Reaction of PUU virus Vero-infected cells with convalescent-phase human sera. Note staining of several cells. (APAAP; original magnifications: A, ×100; B and C, ×250).*

known before this outbreak (Table 2, Figure 2). The staining pattern of MAbs was characteristically punctate, except for the MAbs against SEO virus, which gave more of a diffuse and linear pattern. Human convalescent-phase sera from patients with the acute respiratory illness also reacted specifically with hantavirus-infected cell lines to various degrees (Table 2, Figure 1C). When tested on human tissues from the outbreak, hantaviral antigens were detected in case patients by using the GB04-BF07 MAb that had been shown to cross-react with all known hantaviral serotypes. Localization was primarily within the
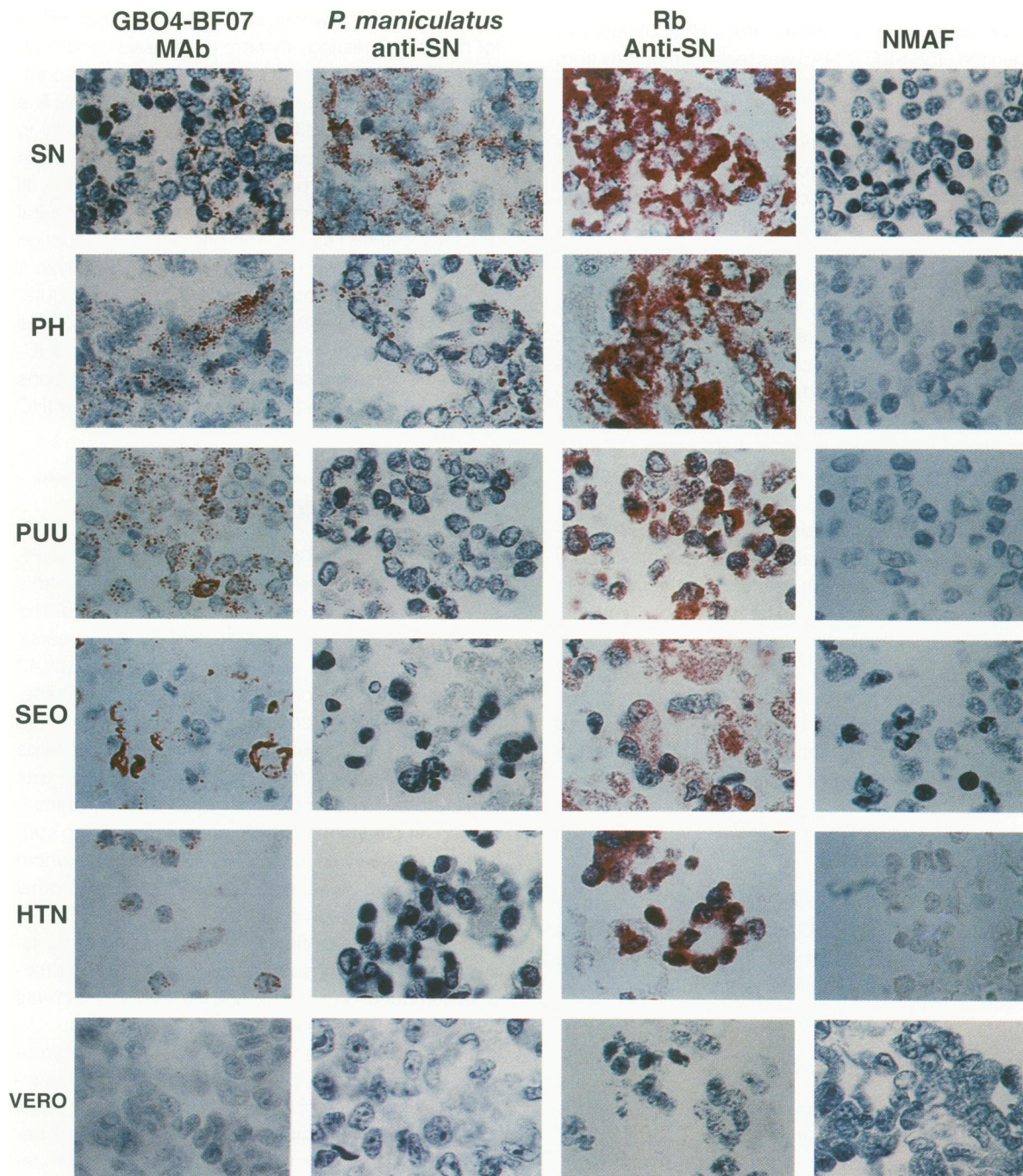
Figure 2. *Immunoalkaline phosphatase staining of hantavirus-infected and noninfected cells with different primary antibodies. The cell lines and antibodies used are indicated. Note reactivity of GB04-BF07 with all hantaviral strains and intense staining of SNV-infected cells with P. maniculatus sera. Less intense staining is seen with both PH and PUU, and no staining with SEO or HTN virus-infected cells. Abbreviations: SN, Sin Nombre; PH, Prospect Hill; PUU, Puumala; SEO, Seoul; HTN, Hantaan; Rb Anti-SN, rabbit anti-serum against SN virus; NMAF, normal mouse ascitic fluid. (APAAP; original magnification ×250).*

capillary endothelium (Figure 3, A and B). All other antibodies initially tested, including convalescent-phase sera, polyclonal antibodies, and all other hantavirus-specific MAbs, failed to detect any antigens in case patients. The GB04-BF07 MAb, after absorption with excess hantaviral antigens, failed to react with tissues from patients with HPS. Immunostaining was not observed when isotype-identical MAbs were used on tissues from HPS patients or when the GB04-BF07 MAb was tested on tissues from patients who died of other illnesses (Figure 3, C and D).

Identification of the deer mouse (P. maniculatus) as the primary rodent reservoir for the new hantavirus[2,7] prompted us to use pooled sera from infected P. maniculatus to study the reaction pattern with control cells and human tissues and to confirm findings obtained with the GB04-BF07 MAb. Of the previously known hantaviral serotypes, the high-titered serum reacted only with PH and PUU virus-infected cells. The pattern of immunostaining of tissues from HPS patients was identical to that observed with GB04-BF07 MAb. No staining was observed with SEO or HTN viruses or noninfected Vero cells and non-HPS cases (Table 2, Figure 2) or when sera from serologically negative rodents were used.

Once the new hantavirus (SNV) was isolated in culture, polyclonal rabbit antisera were prepared. The polyclonal rabbit antisera reacted with tissues from HPS patients in a pattern similar to that observed with the GB04-BF07 MAb and the pooled P. maniculatus sera. However, in addition, staining of lymphoreticular cells was a more prominent finding (see below). The reaction of GB04-BF07, high-titered P. maniculatus serum, and polyclonal rabbit sera with SNV-infected cells are shown in Figure 2.

Hantaviral Serology

One hundred and fifty serum samples were tested by using IgG and IgM ELISAs. Thirty-two specimens showed evidence of recent infection, three were equivocal, and the remainder were negative.

Hantaviral RNA Detection

Sixty-one human samples were tested by using the RT-PCR assay. Positive virus-specific PCR-amplified DNA bands were visualized from 26 of the tested samples. In each case, the authenticity of the amplified products was confirmed by the excision of the DNA bands from the agarose electrophoresis gels and by direct nucleotide sequence analysis. All PCR-

positive samples reported here had sequences compatible with SNV.

Concordance of IHC, Serology, and PCR Test Results

Of the 273 patients with unexplained noncardiogenic pulmonary edema whose specimens were submitted for hantavirus testing, 43 were diagnosed as HPS on the basis of results from IHC analysis alone or in combination with serology and/or RT-PCR (Table 3). The results of the three different assays were virtually in complete agreement when more than one assay was performed. Of the 44 patients diagnosed with HPS, all but one had unequivocal IHC evidence of hantaviral antigens in their tissues. The one notable exception was patient 6, whose tissues were severely autolyzed, making IHC interpretation impossible. Two acute-phase sera, with weak IgM reactions to homologous and heterologous hantavirus antigens, were IHC-positive. One serum sample, with weak IgM reactions to SEO virus antigens, was not positive by either IHC or PCR.

Clinical and Pathological Findings

Available clinical and laboratory data from the 44 HPS patients are summarized in Table 4. Included in this series of patients were 26 males and 18 females. The median age was 33.5 years (range 14 to 68 years). Exposure to rodents was documented for 22 of 42 patients for whom information was available; of these, 19 had evidence of rodents in the home, which could have brought them into contact with aerosolized virus shed by rodents. Information about occupation was available for 35 patients, of whom 10 reported animal-related employment, including two persons who specifically worked with rodents. All 42 patients for whom a clinical history was available reported a prodromal illness that had been present for a median of 3 days before medical attention was sought. In 13 patients, the duration of prodrome was 2 days or less. The median number of days from disease onset to death was 4 days (2 to 20 days).

Fever and myalgia were the most common symptoms reported (Table 5). Notable laboratory data included thrombocytopenia with platelet counts of <150,000 in all patients tested and <50,000 in 22 patients (54%). Elevated hematocrit levels (>47% females; >52% males) were reported in 40 (95%) persons tested and neutrophilic leukocytosis with pronounced left shift was present in 29 of 38 patients tested (WBC: median = 20,900; range: 3,100 to
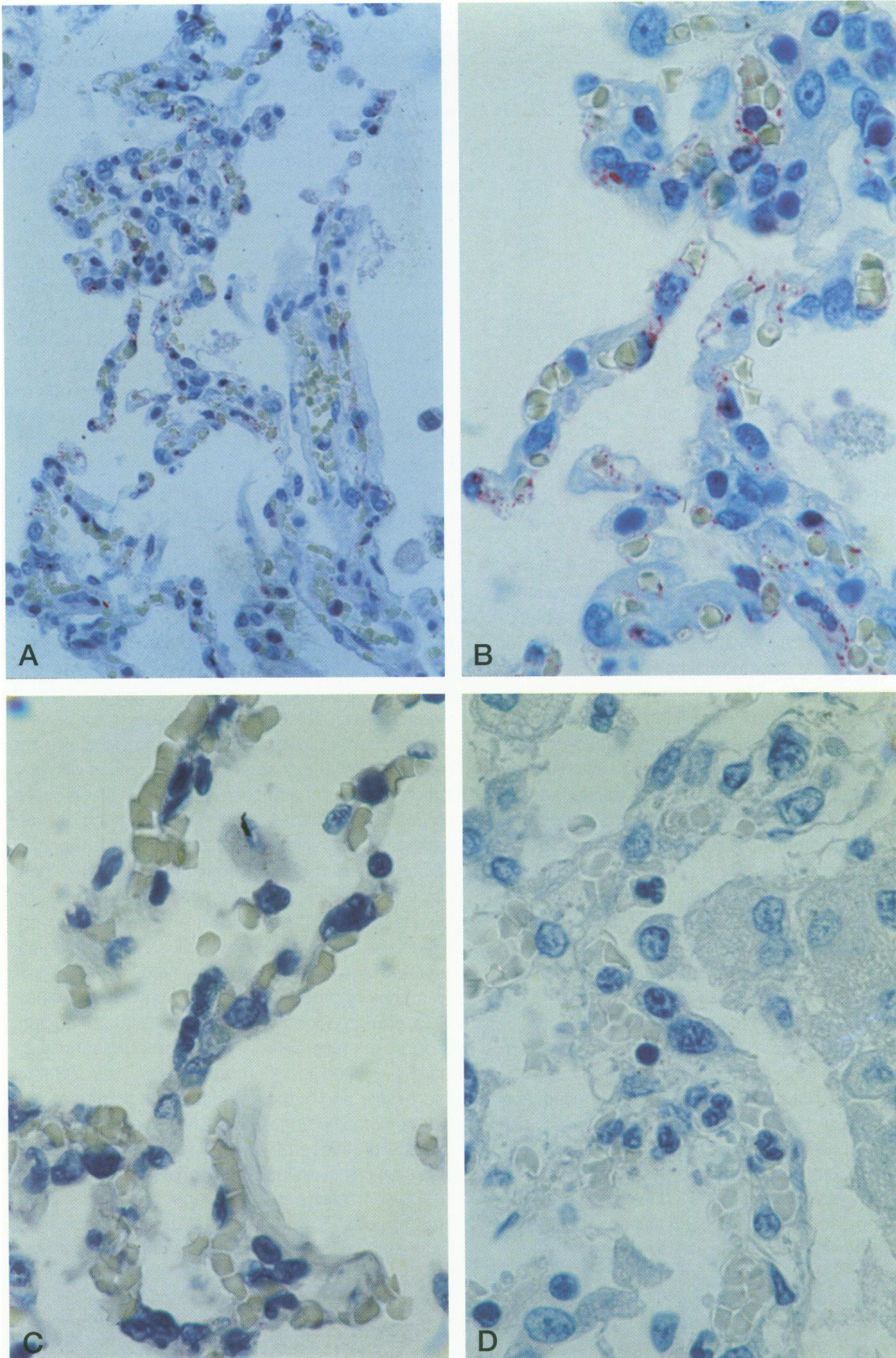
Figure 3. (A, B) *Immunolocalization of hantaviral antigens to pulmonary microvasculature of an HPS patient (case 17) with GB04-BF07 MAb. Note fine punctate staining of capillary walls. (C) Absence of immunostaining of same case using isotype-identical murine control antibody. (D) Absence of immunostaining in a non-HPS case with GB04-BF07 MAb. (Original magnifications: A, ×100; B–D, ×250).*

Table 3. *Summary of Hantavirus Tests Performed on 273 Cases of Unexplained Noncardiogenic Pulmonary Edema*

IHC	Serology	PCR	Total (%)
HPS-positive cases (N = 44)			
+	+	+	24 (55)
+	+	ND	6 (14)
+	ND	ND	9 (20)
+	+/−	ND	2 (5)
+	+	−	1 (2)
+	ND	+	1 (2)
Inadequate*	+	+	1 (2)
HPS-negative cases (N = 229)			
−	−	−	26 (11)
−	−	ND	85 (37)
−	ND	ND	102 (45)
−	ND	−	7 (3)
Inadequate*	−	ND	4 (2)
Inadequate*	ND	ND	4 (2)
−†	+/−	−	1 (0.4)

*Inadequate (autolyzed) tissue for IHC analysis.
†Patient with low-level SEO IgM reaction on several acute sera, no convalescent sera available for follow-up serology.
ND, Not done.

71,900). Proteinuria ($\geq 2+$) was seen in 13 of 28 patients tested. Serum creatinine levels were elevated (>1.3 for males; >1.2 for females) in 21 of 38 persons tested. Prolongation of the prothrombin time (PT > 13 s) and the partial thromboplastin time (PTT > 34 s) was observed in 17 of 21 patients tested. In 8 of 10 patients with prolonged PT and PTTs, fibrin split product or D-dimer assays were positive. Fibrinogen levels were available for seven of these patients and were found to be decreased in two. Despite laboratory findings strongly suggesting the occurrence of disseminated intravascular coagulopathy (DIC) in eight patients and consistent with DIC in many others, overt clinical signs of hemorrhage were rarely reported. Arterial blood gas results were reviewed for 21 patients who were intubated and given 100% supplemental oxygen. Highest pO_2 levels ranged from 4.2 to 79 mm Hg (median 52) and coincided with corresponding pCO_2 levels and pH ranging from 25 to 124 mm Hg (median 36) and 6.68 to 7.42 (median 7.22), respectively. Radiographic findings among these same 21 patients included bilateral pulmonary infiltrates in all cases and pleural effusions in six cases. Despite the absence of radiographic evidence for pleural effusion before death, an additional seven patients were later found to have copious pleural effusions at postmortem examination.

Multiorgan involvement was noted in all 44 fatal cases of HPS with variable degrees of generalized vascular congestion; however, the main histopathological features were seen primarily in the lung. Vascular thrombi and endothelial cell necrosis were ab-

sent. In fact, morphological changes of endothelium were uncommon and, when present, consisted of prominent and swollen endothelial cells. Focal microscopic hemorrhages in various organs were exceedingly rare, and ischemic necrotic lesions, except those attributed to shock, were not seen.

In most cases (40/44), microscopic examination of the lung revealed a mild to moderate interstitial pneumonitis with variable degrees of congestion, edema, and mononuclear cell infiltration (Figure 4, A and B). The cellular infiltrate was composed of a mixture of small and enlarged mononuclear cells with the appearance of immunoblasts. Extensive amounts of edema fluid and fibrin as well as variable numbers of inflammatory cells were seen within the alveoli. In the majority of these cases, focal hyaline membranes were observed. These membranes were poorly formed in most instances and were primarily composed of condensed fibrin apposed to the alveolar wall. The contribution of neutrophils to the cellular response in these typical cases was minimal. Moreover, the respiratory epithelium was intact with no evidence of cellular debris, nuclear fragmentation, or type II pneumocyte hyperplasia. Less common histological features were observed in four HPS cases. In three of these cases (patients 19, 23, and 36), there were variable degrees of more typical dense-laminated hyaline membranes and proliferation of reparative type II pneumocytes. This was accompanied by severe edematous and fibroblastic thickening of the alveolar septa and severe air space disorganization with distortion of the lung architecture in two of these cases (Figure 5). These three patients were among only six patients who survived more than 2 days in the hospital before death. In a fourth patient (patient 43), there was a variation in the histological appearance of the lung among the different blocks and fields examined. Whereas some fields showed typical HPS histological features, other areas showed an intense intraalveolar inflammatory process with large numbers of neutrophils, and red blood cells enmeshed in a coagulum of fibrin. In these areas, the intense purulent inflammation resulted in extensive cellular fragmentation and destruction of the alveolar septa (Figure 5).

A common finding seen in all the cases examined was the presence of variable numbers of immunoblasts within the red pulp and periarteriolar sheaths of the spleen, and paracortex and within sinuses of lymph nodes (Figure 4, C and D). Mononuclear inflammatory cells with occasional immunoblasts were seen in the portal triads of most cases. Clusters of hypertrophic and hyperplastic Kupffer cells containing cellular debris were seen filling the hepatic sinusoids in a few cases. Bone marrow examination re-

Table 4. *Forty-four Patients with Fatal Hantavirus Pulmonary Syndrome: Available Clinical and Laboratory Data*

Case	Age (yr), sex	Pro-drome (days)	Days to death	Platelets*	% HCT[†]	WBC	Band	PMN	Lymph	Mono	Eos	Proteinuria	Creatinine
1	33 F	2	3	64,000	58	37.2	52¶	23	17	0	0	3+	1.3
2	21 F	7	8	148,000	53	10.4	65	24	7	4	0	Trace	0.8
3	19 M	2	3	42,000	60	65.3	27¶	45	17	0	2	–	2.5
4	58 F	10	11	93,000	56	11.4	10¶	53	30	7	0	1+	1.1
5	21 M	1	2	54,000	58	53.4	49¶	29	10‖	4	1	–	1.7
6	31 M	2	3	NA	NA	NA	NA	NA	NA	NA	NA	NA	NA
7	22 F	4	7	98,000	46	3.9	4	58	32	6	0	2+	0.7
8	34 M	5	6	25,000	56	20.7	18¶	64	13‖	0	0	3+	"Normal"
9	22 F	1	2	58,000	49	13.2	53¶	34	7	0	2	2+	0.5
10	64 F	2	4	73,000§	48	14.1	12	79	4	3	2	2+	0.1
11	35 F	5	6	62,000	48	4.4	26	51	19	2	2	–	0.9
12	39 F	7	9	28,000§	52	3.1	22	49	24‖	5	0	–	0.5
13	42 F	4	4	NA	52	12.6		80	10	10	0	NA	NA
14	34 M	4	4	21,000	68	31.7	10¶	68	15	4	1	3+	0.2
15	29 M	3	3	98,000	59	20.3	66¶	21	6	5	0	NA	0.5
16	16 M	3	3	10,000§	58	37.8	34	30	8‖	8	1	4+	0.2
17	68 M	7	10	14,000	56	23.1	32	52	4‖	4	0	–	1.2
18	27 F	2	3	16,000§	62	11.6	29¶	46	20‖	2	0	–	1.8
19	64 F	4	20	24,000	60	30.7	45¶	19	19‖	15	2	4+	4.2
20	14 M	3	3	45,000	58	35.5	32	27	30	8	3	NA	2.1
21	34 M	5	5	59,000	56	16.4		70	12	17	0	NA	1.7
22	35 M	7	9	12,000§	65	18.9	35	43	22	0	0	Trace	1.2
23	22 M	4	20	25,000§	53	20.1	31	52	17‖	0	0	Trace	0.9
24	45 F	3	3	28,000	62	20.9	30	50	12	7	1	2+	2.4
25	26 M	3	3	24,000	77	26.1	8	74	18	0	0	NA	2.6
26	22 M	4	4	55,000	70	23.2	37	59	NA	NA	NA	NA	1.8
27	34 F	5	6	13,000	66	71.9	21¶	32	12	12	0	1+	0.9
28	38 M	2	3	63,000	58	10	3¶	79	14‖	2	1	NA	3.5
29	14 M	2	3	38,000	42	41.5	20¶	43	14	17	0	NA	2
30	30 M	3	4	52,000	60	13.3	11	63	26	0	0	NA	NA
31	18 F	2	2	11,000	49	28.9	2	63	31	4	0	2+	1.4
32	22 M	4	6	34,000	56	14.3	11¶	61	10	15	2	2+	1.9
33	48 M	2	3	102,000	53	50.5	31¶	55	5‖	7	0	NA	1.4
34	22 M	3	3	61,000	50	7.4	41	31	17‖	5	0	Trace	1.1
35	20 M	5	7	17,000	67	45	34¶	45	9‖	0	2	1+	1.8
36	49 F	3	19	61,000§	51	20.3	42¶	34	16‖	4	0	NA	1
37	31 M	4	5	75,000	61	21.3	15	69	16	0	0	1+	1.6
38	27 F	2	4	102,000	50	7.4	3¶	83	13‖	0	1	2+	0.9
39	35 F	2	2	38,000	60	34.6	44	23	21‖	2	0	NA	2.7
40	34 M	NA	NA	69,000	62	33.1	NA	NA	NA	NA	NA	NA	NA
41	36 M	NA	NA	18,000	66	NA	NA	NA	NA	NA	NA	NA	NA
42	55 M	7	13	18,000	65	37	25¶	40	20	3	3	2+	1.9
43	35 M	7	9	47,000§	65	29.3	39	49	11	1	0	–	1.2
44	34 F	3	4	NA	NA	NA	NA	NA	NA	NA	NA	NA	NA

*Minimum platelet count (mm^{-3}) recorded.
[†]Maximum hematocrit (%) recorded.
[‡]Band = neutrophilic bands; PMN = polymorphonuclear leukocytes; Lymph = lymphocytes; Mono = monocytes; Eos = eosinophils.
¶Band precursors noted.
§These patients had prolonged PTs and PTTs and evidence of fibrin split products (D-dimers).
‖Atypical lymphocytes noted.
NA = not available; WBC = white blood cell count × 10^3/mm^3.

vealed a moderate increase in cellularity with prominent left-shifted myelopoiesis. A slight increase in the number of normal-appearing megakaryocytes and minimal hemaphagocytosis was also seen.

Immunophenotyping of Inflammatory Cells

Characterization of the pulmonary mononuclear cell infiltrate was undertaken in five HPS patients. In all five cases, the infiltrate was shown to be composed mainly of a mixture of T lymphocytes (CD3-positive) and macrophage/monocytic cells (KP1- and Ki-M1P-

positive) (Figure 6). Only rare B lymphocytes (L26-positive) were noted. When the T-cell subpopulations in the lung were examined in frozen tissue sections, the CD4/CD8 ratio varied from 1.2 to 2.

Cellular Targets and IHC Distribution of SNV Antigens

Immunohistochemical evidence for the presence of hantaviral antigens was documented in tissues from all the patients with HPS. In all cases, immunostaining was observed by using both the GB04-BF07 MAb and

Table 5. *Frequency of Reported Prodromal Symptoms for 42 Fatal HPS Cases*

Symptom	No. (%)
Fever	41 (98)
Myalgias	24 (57)
Vomiting	18 (43)
Weakness/Fatigue	14 (33)
Cough	13 (31)
Diarrhea	12 (29)
Nausea	12 (29)
Shortness of breath	11 (26)
Headache	10 (24)
Dizziness	5 (12)
Rhinorrhea	4 (10)
Abdominal pain	3 (7)
Chest pain	3 (7)
Numbness (digits, extremities)	2 (5)

the high-titered polyclonal sera from infected *P. maniculatus*. Viral antigen-positive cells were widely distributed in various tissues examined, including lung, kidney, heart, spleen, pancreas, lymph node, skeletal muscle, intestine, adrenal gland, adipose tissue, urinary bladder, and brain (Figures 7 to 9). The appearance of SNV antigens was characteristically finely granular and seen predominantly within endothelial cells of capillaries and small vessels. Viral antigens were rarely detected in endothelial cells of large veins or arteries. The endothelial cells were clearly identified by their location and pattern of staining. Double staining for SNV antigens along with antibodies to either FVIII or CD31 confirmed the identity of these SNV antigen-positive cells as endothelial cells (Figure 10, A–C). In all cases, the most intense and extensive endothelial immunostaining of viral antigen was observed in tissue sections from the lung. The antigen-positive endothelial cells in the lung were usually abundant, uniformly distributed, and involved most of the pulmonary microvasculature. In cases in which tissues from various segments of the lungs were available for IHC analysis, no variation in the amount or extent of endothelial immunostaining was seen. In the few HPS cases with longer survival intervals, lesser amounts of antigen were detected in both endothelial cells and macrophages (Figure 7F). The kidneys showed prominent but less extensive endothelial presence of SNV antigens. Staining was seen primarily in the interstitial capillaries of the medulla, and to a lesser degree, in those of the cortex (Figure 8, A and B). Glomerular endothelial cells also showed focal immunostaining (Figure 8C). Staining of tubular epithelial cells was a rare finding.

The amount and extent of endothelial immunostaining was less consistent in other organs, with considerable variation among cases. All heart, spleen, brain, skeletal muscle, intestinal, and pancreatic tissues examined demonstrated some evidence of endothelial immunostaining. In the heart, endothelial staining was mainly in the capillaries of the myocardium (Figure 8D) and varied from focal immunostaining in some cases to diffuse and extensive staining in others. Occasionally, staining of endothelial cells lining the endocardium was observed (Figure 8E). In the spleen, immunostaining was usually observed primarily in sinus lining cells of the red pulp and occasionally in endothelial cells lining central arterioles and other large vessels (Figure 9A). In lymph nodes, endothelial staining was mainly seen in the subcapsular area. The organ in which evidence of staining was most difficult to find was the liver. In the majority of liver specimens examined, only rare sinusoidal lining cells demonstrated focal positivity (Figure 9B).

High densities of SNV antigens were also observed in lymphoid follicles of the spleen and, to a lesser extent, in lymph node follicles (Figure 11, A and B). The staining was delicate and reticular in nature and was seen in the majority of spleen tissue specimens examined. The strongest staining was seen with rabbit polyclonal anti-SNV sera. *Peromyscus* serum gave moderate staining, and the GB04-BF07 MAb, showed weaker but definitely positive staining. The topographical relationship of SNV antigens and follicular dendritic cells (FDCs) was analyzed in select cases by immunostaining of serial sections of the spleen and lymph nodes. Deposits of SNV antigens occurred in a pattern identical to that of FDC labeling, with the majority of identifiable FDCs exhibiting SNV staining (Figure 12, A and B). Viral antigen was also found in a low percentage of large cells, identified morphologically as macrophages, in the lung, splenic sinusoids, and bone marrow (Figures 7 and 11). Some of these cells contained engulfed necrotic debris. In a few cases, hypertrophic Kupffer cells containing SNV antigens and phagocytosed debris were seen within hepatic sinusoids (Figure 11C). Cells with the appearance of lymphocytes were occasionally seen to contain SNV antigens (Figure 7D).

Electron Microscopy and Immunoelectron Microscopy

EM examination of lung autopsy tissues of HPS patients showed evidence of interstitial edema with

---

Figure 4. *Photomicrographs showing histopathological features in a typical case of HPS (case 14).* (**A**) *Low-power photomicrograph showing interstitial pneumonitis and intraalveolar edema.* (**B**) *Higher magnification showing intraalveolar fibrin deposits and mononuclear cellular infiltrate.* (**C, D**) *Immunoblasts in the periarteriolar sheath of the spleen. Note prominent nucleoli and high nuclear to cytoplasmic ratio.* (*Original magnifications:* **A**, ×50; **B** *and* **C**, ×100; **D**, ×250).
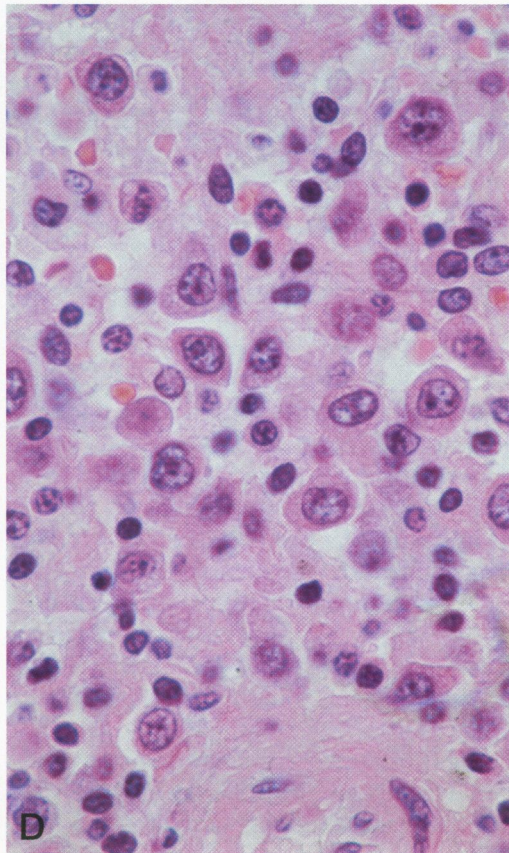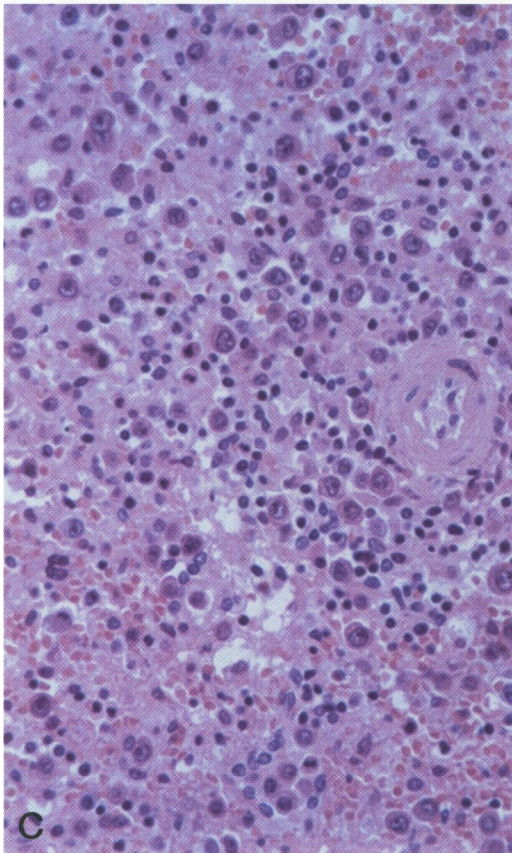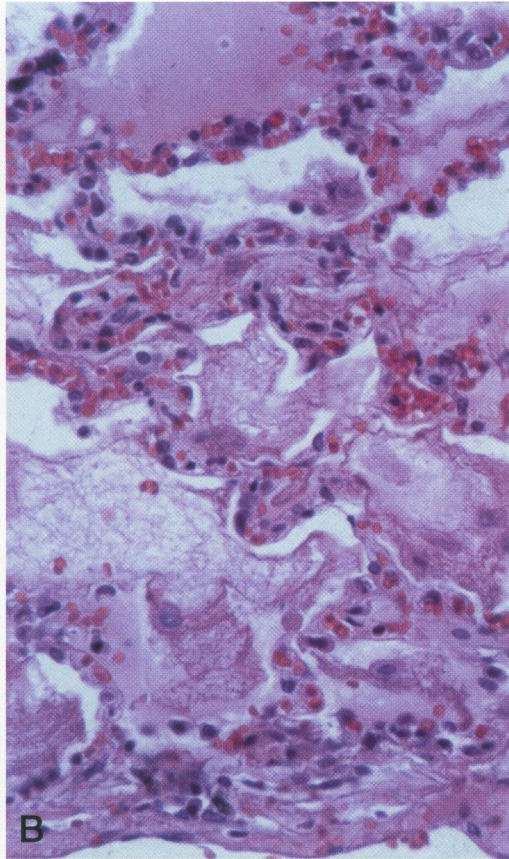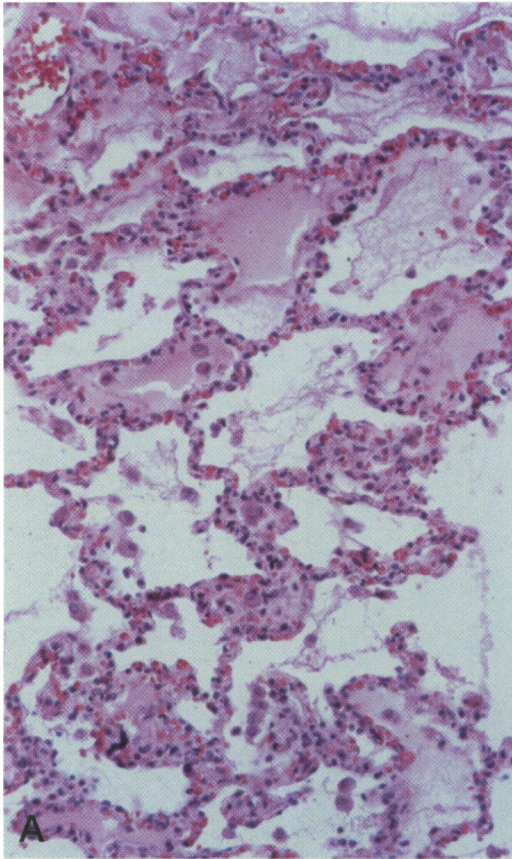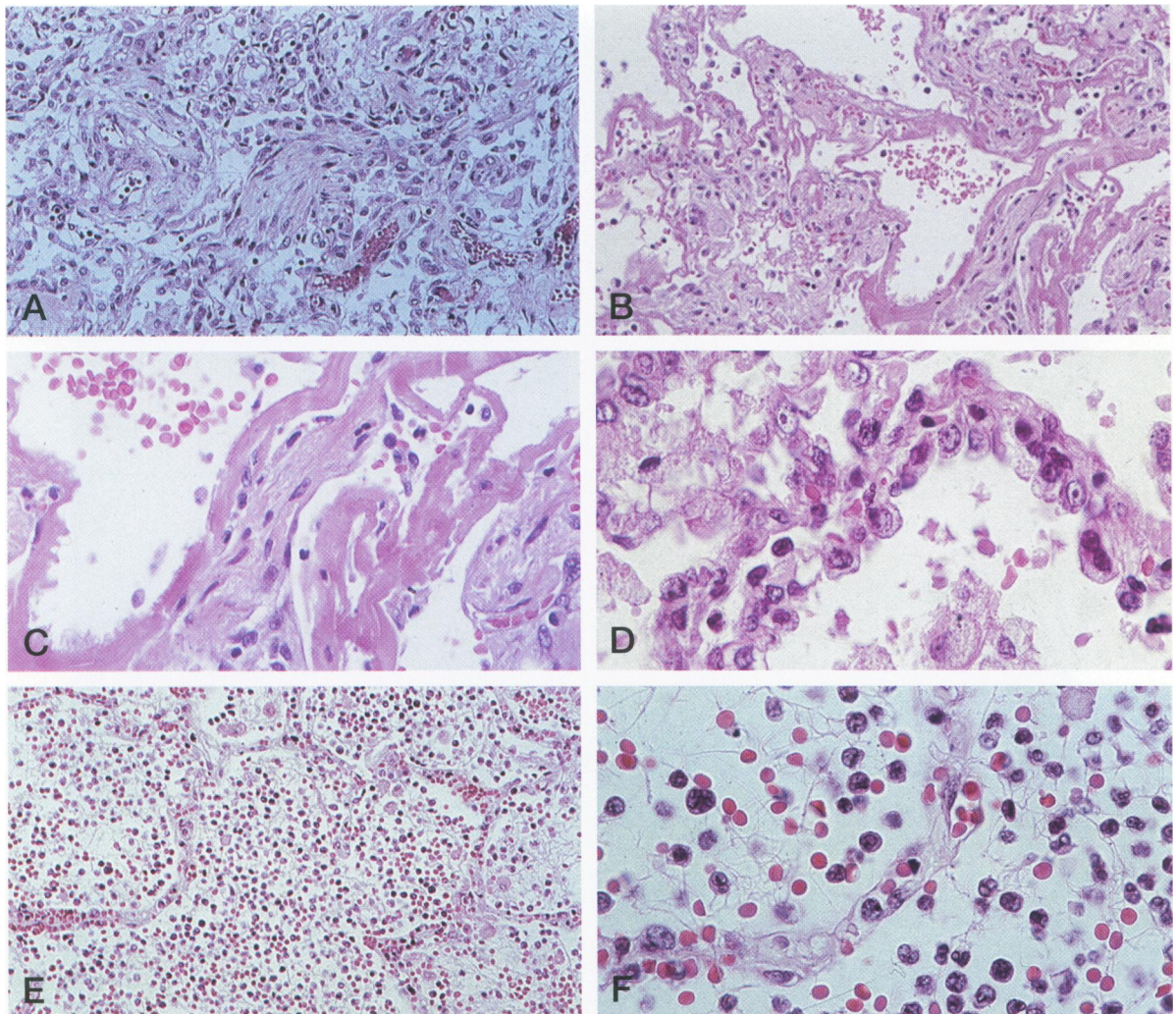
Figure 5. *Photomicrographs showing histopathological features less commonly seen in cases of HPS.* (**A**) *Case 23. Lung showing extensive interstitial and alveolar fibrosis. Note the increased interstitial cellularity with numerous fibroblasts.* (**B**) *Case 36. Photomicrograph showing patchy areas of alveolar septal thickening and prominent hyaline membranes.* (**C**) *Case 36. Higher magnification showing typical dense laminated hyaline membranes.* (**D**) *Case 36. Alveolar septum showing prominent type II pneumocyte proliferation.* (**E**) *Case 43. Abundant polymorphonuclear leukocytes fill alveolar spaces with focal destruction of alveolar septa.* (**F**) *Case 43. Higher-power magnification showing the intraalveolar exudate composed mainly of polymorphonuclear leukocytes, red blood cells, and fibrin.* (*H&E; original magnifications:* **A** *and* **B**, ×50; **C**, ×100; **D**, ×158; **E**, ×50; **F**, ×158).

distorted and slightly thickened basement membranes. Abundant inflammatory cells, some with morphological features of activation, were seen within capillary lumina, interstitium, and alveoli. The alveolar spaces also contained dense accumulations of fibrin. The endothelial cells appeared slightly swollen and mostly intact. Occasionally, the continuity of the endothelial cells lining the capillaries, as well as the epithelial cells along the basement membranes, was interrupted. It must be noted, however, that the latter changes were probably a result of postmortem autolysis.

Within the cytoplasm of some pulmonary endothelial cells, typical hantavirus inclusions were observed, consisting of granular, filamentous, or granulofila-

mentous material.[20,21] These inclusions varied in shape from small and spherical, measuring as little as 0.2 μ in diameter, to more oblong inclusions, measuring up to 2.1 μ in the longest dimension (Figure 13). The inclusion bodies were usually seen within the perinuclear region of the endothelial cell. The viral nature of these inclusions was confirmed using immunogold EM with either *Peromyscus* serum or the GB04-BF07 MAb (Figure 14).

Single hantavirus-like particles were found in a few endothelial cells within the pulmonary microvasculature. In addition, collections of whole virus-like particles were found in association with interstitial macrophages in lung autopsy tissue from one of the HPS patients (Figure 15). These enveloped particles were
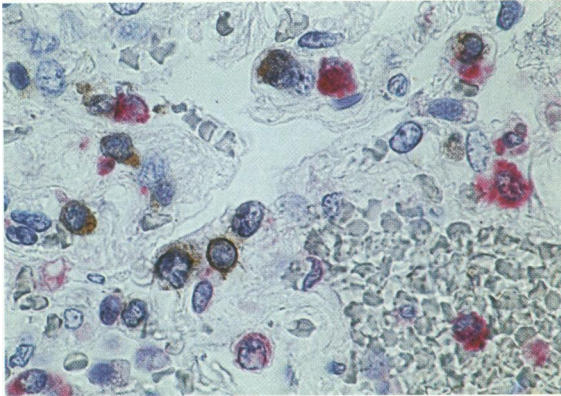
Figure 6. *Immunophenotyping of inflammatory cells in lung of an HPS patient (case 38) by double staining for monocyte/macrophage and T-cell markers. Note that most cells label with either monocyte/macrophage marker (Ki-M1P⁺, alkaline-phosphatase/red) or T-cell marker (CD3⁺, peroxidase/brown). (Original magnification, ×250).*

roughly spherical and contained a dense homogenous core which filled the particle. The particles were much more compact than the virus grown in tissue culture,[22] averaging only 58 nm. These accumulations of particles within the macrophages were occasionally associated with phagolysosomes containing fragments of cellular debris.

Discussion

A previously unrecognized hantavirus, SNV, was recently isolated and identified as the cause of an outbreak of a severe respiratory disease in the southwestern United States. Early in this outbreak, the discovery of a serological link between known hantaviruses and this new and unexplained syndrome resembling adult respiratory distress syndrome (ARDS)[2,17] was received with some degree of uncertainty. In spite of our confidence in the validity of the serological test based on extensive experience with serological evaluation of hantavirus infections in countries such as Yugoslavia, Sweden, Korea, and China,[23] these patients resided in a geographical area with no previously documented hantavirus disease, manifested a syndrome not previously associated with hantavirus infection, and had a pattern of serological reactivity that was not typical of any of the known hantaviruses. Initially, by examining coded specimens, we were able to correlate the histopathological features of fatal cases with serological evidence of hantavirus infection. Although this correlation led to increased confidence of the diagnosis during the first few days of the laboratory investigation, additional confirmation was needed to identify the nature of the hantavirus and establish an etiological relationship. Within less than a week, amplification

of genetic sequences from autopsy material and demonstration of viral antigens in tissues from HPS patients established a previously unrecognized hantavirus as the causative agent.[3,5,6]

The initial symptoms of HPS in these fatal cases resemble those previously reported[15] and are similar to the early phases of many other viral diseases. The abrupt onset of respiratory failure and shock, however, is an unusual feature that presented a diagnostic and therapeutic challenge. The duration of the prodrome in fatal cases included in this series was typically about 3 days (median), and 86% of the patients died within 2 days of hospitalization. All the patients had the typical hematological findings of thrombocytopenia, and most had hemoconcentration (95%) and neutrophilic leukocytosis with a left shift (76%). This clinical picture is quite different from that of HFRS due to HTN virus infection, in which renal failure is common but pulmonary edema early in infection is unusual. Only HFRS patients who died during the later phase of renal failure typically showed substantial pulmonary edema.[24] HFRS is associated with more generalized signs of nondependent edema, and the major focus for fluid transudation is the retroperitoneal space.[24,25] Uncommonly, patients with HFRS caused by HTN virus presented early with severe pulmonary edema,[26,27] but even in these situations, therapeutic overhydration may have been a factor.[25] Careful examination of the lungs and chest cavity with CT scanning confirms the regular involvement of the lungs and pleural cavity in the mild form of HFRS associated with PUU virus infection.[28] Other obvious differences between HTN virus and SNV infection include the higher frequency of peripheral signs of vasomotor instability, such as flushing and conjunctival injection, and hemorrhagic manifestations in HFRS. Hemorrhage, at least at the level of petechiae, occurs in at least one-third of patients with HFRS due to PUU virus, whereas virtually all patients with HFRS associated with HTN virus will have petechiae and most will have severe hemostatic difficulties.[29–31] Despite the thrombocytopenia, high mortality, and severity of pulmonary compromise associated with HPS, clinical bleeding was an uncommon finding in our series. However, there are some marked similarities between HPS and severe HFRS, including the circulatory status (shock with decreased cardiac output, increased systemic vascular resistance[15,32]), leukocytosis, presence of atypical lymphocytes,[33] and the common feature of lesions with marked permeability in at least some microvascular beds.

The utility of IHC as a diagnostic modality was established by the virtual concordance with results of the two other laboratory tests for hantavirus infection,
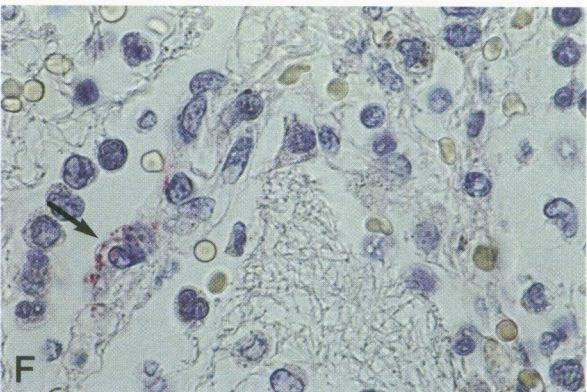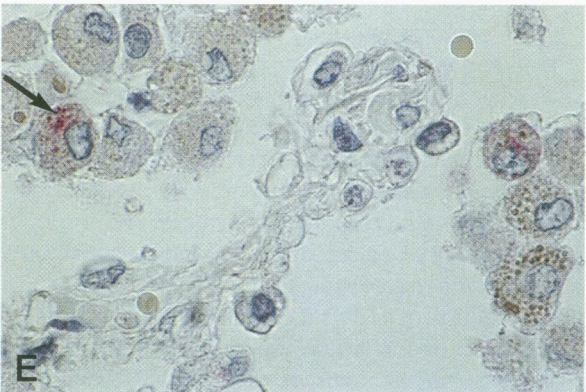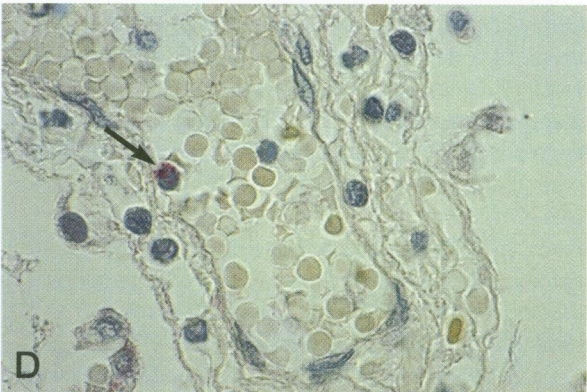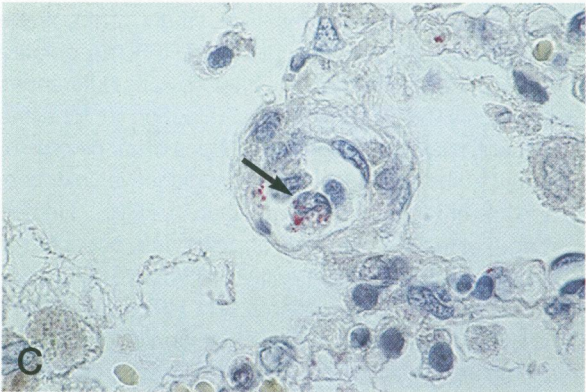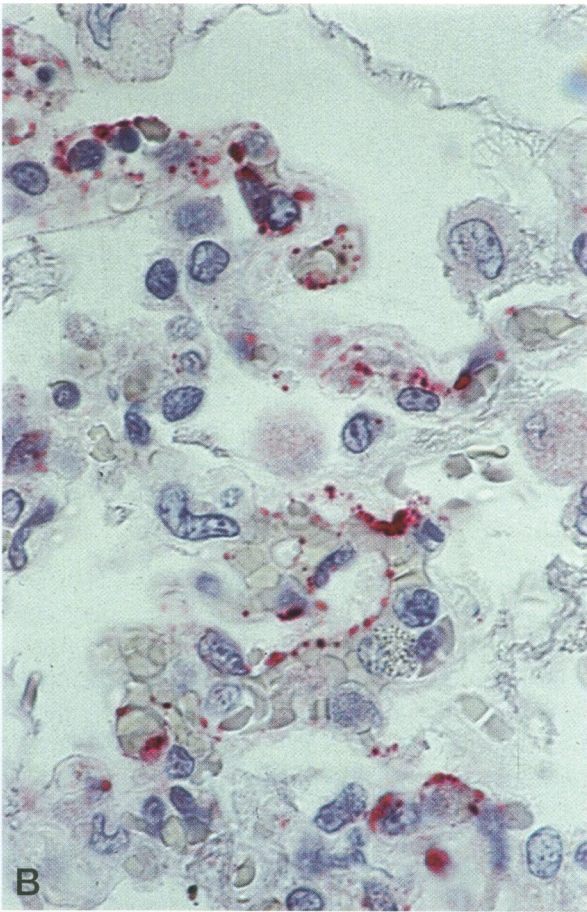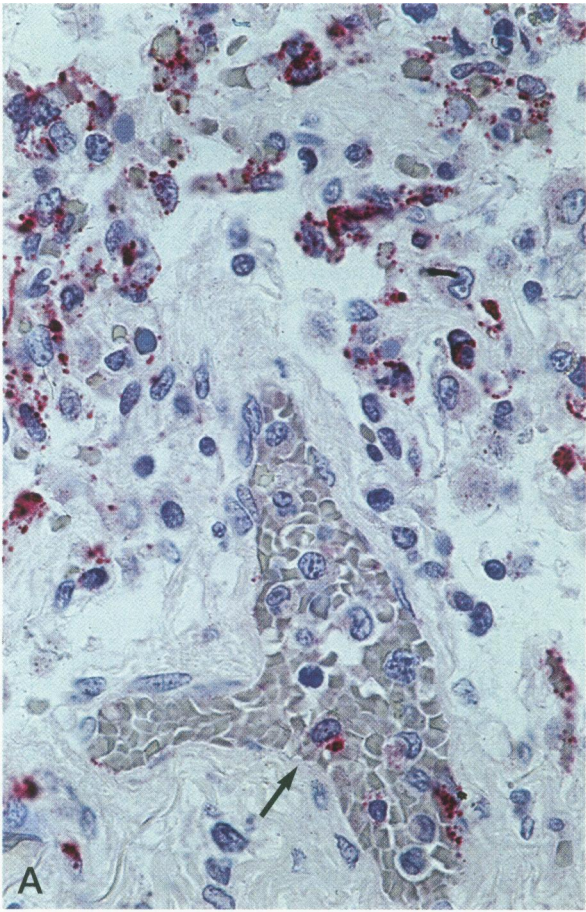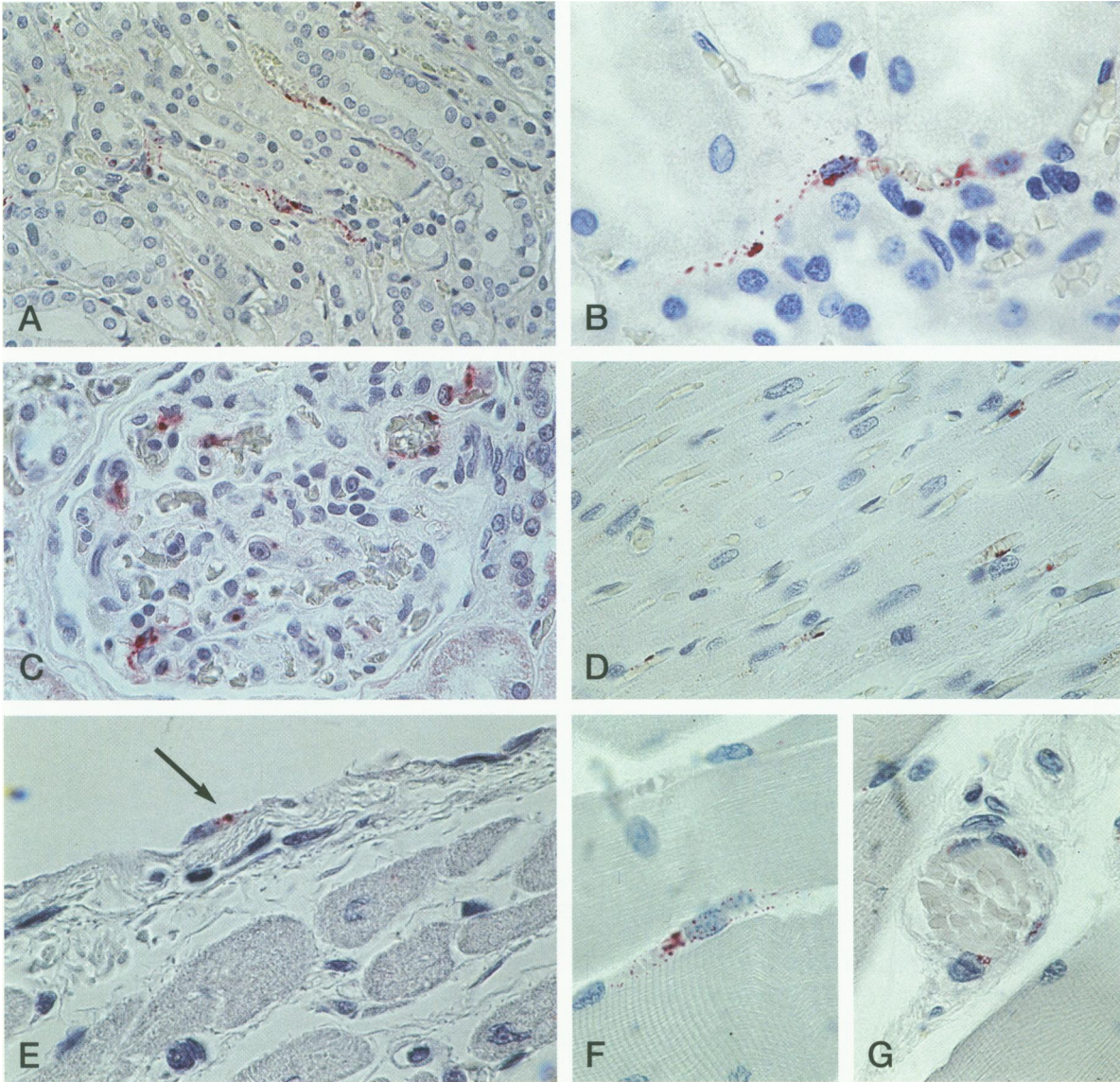
Figure 8. (A) *Case 38. Prominent endothelial staining in interstitial capillaries of the renal medulla. Note absence of tubular staining. Rabbit anti-SNV serum.* (B) *Case 28. High-power magnification showing immunostaining of renal interstitial capillaries using immune* Peromyscus *serum.* (C) *Case 38. Focal SNV antigens within glomerular endothelial cells. Rabbit anti-SNV serum.* (D) *Case 38. Staining of several capillaries in myocardium. GB04-BF07 MAb.* (E) *Case 38. A rare SNV antigen-positive endothelial cell lining endocardium is seen (arrow). GB04-BF07 MAb.* (F, G) *Case 17. SNV antigens within skeletal muscle capillaries as seen in longitudinal (F) and transverse (G) sections. GB04-BF07 mAb. (Original magnifications: A, × 100; B, × 250; C and D, × 158; E–G, × 250).*

IgM ELISA and RT-PCR, when one or both of the additional assays were used. Several antibodies were initially evaluated for use in IHC assays, and one MAb was selected because of its broad reactivity in formalin-fixed tissues. As new reagents were developed, they were evaluated and used as confirmatory tools and for research purposes. Hyperimmune rabbit serum was found to be a valuable component because of its high specificity and broad reactivity. The pattern of reactivity of antibodies used in the study, in particular the *Peromyscus maniculatus* serum, with cell lines and human tissues, suggests that SNV is

Figure 7. *SNV antigen-positive cells in lungs of HPS patients as determined by immunohistochemistry.* (A) *Case 38. Low-power magnification showing predominantly endothelial staining in pulmonary microvasculature. Note, however, staining of at least one intravascular mononuclear cell (arrow). Rabbit anti-SNV serum.* (B) *Higher magnification showing fine granular immunostaining of SNV antigens along capillary walls. Rabbit anti-SNV serum.* (C) *Case 44. High-power magnification showing SNV antigens within an intravascular mononuclear cell with the appearance of a monocyte (arrow). Immune* Peromyscus *serum.* (D) *Case 44. An SNV antigen-positive cell, most likely a lymphocyte, within a pulmonary vessel (arrow). GB04-BF07 MAb.* (E) *Case 44. SNV antigen-positive intraalveolar macrophages (arrow). GB04-BF07.* (F) *Case 43. Focal endothelial staining as seen in an uncommon histological form of HPS (arrow). GB04-BF07. (Original magnifications: A, × 158; B–F, × 250).*
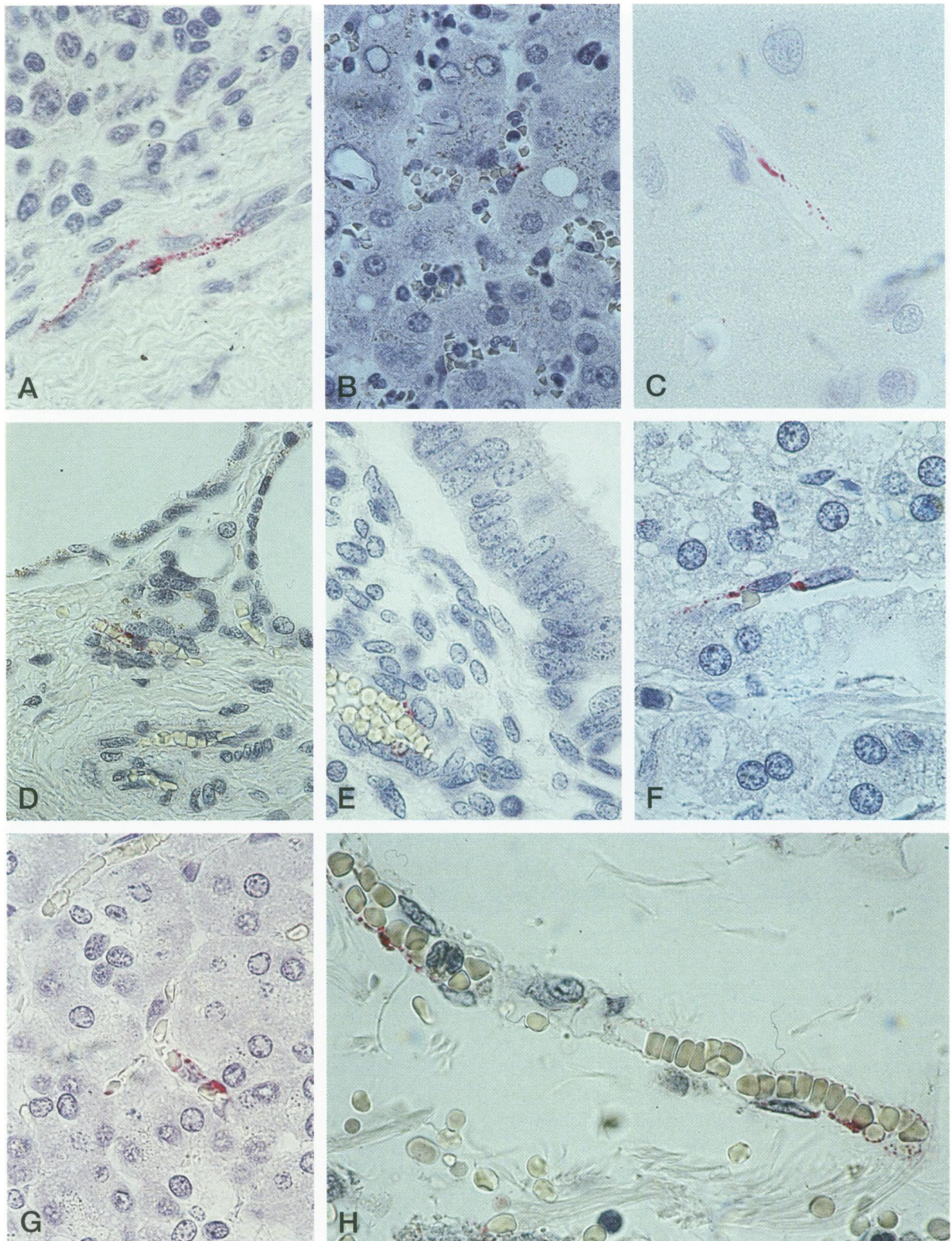
Figure 9. *Immunostaining of viral antigen in endothelial cells in various organs as determined by immunohistochemistry.* (**A**) *Spleen of case 38. GB04-BF07 MAb.* (**B**) *Liver of case 38. Rabbit anti-SNV serum.* (**C**) *Brain of case 6. GB04-BF07 MAb.* (**D**) *Thyroid of case 11. Immune* Peromyscus *serum.* (**E**) *Endometrium of case 11. GB04-BF07 MAb.* (**F**) *Adrenal of case 12. GB04-BF07 MAb.* (**G**) *Pancreas of case 39. GB04-BF07 MAb.* (**H**) *Retroperitoneal adipose tissue of case 21. Immune* Peromyscus *serum.* (*Original magnifications:* **A**, ×250; **B**, ×158; **C**, ×250; **D**, ×158; **E–G**, ×250; **H**, ×158).
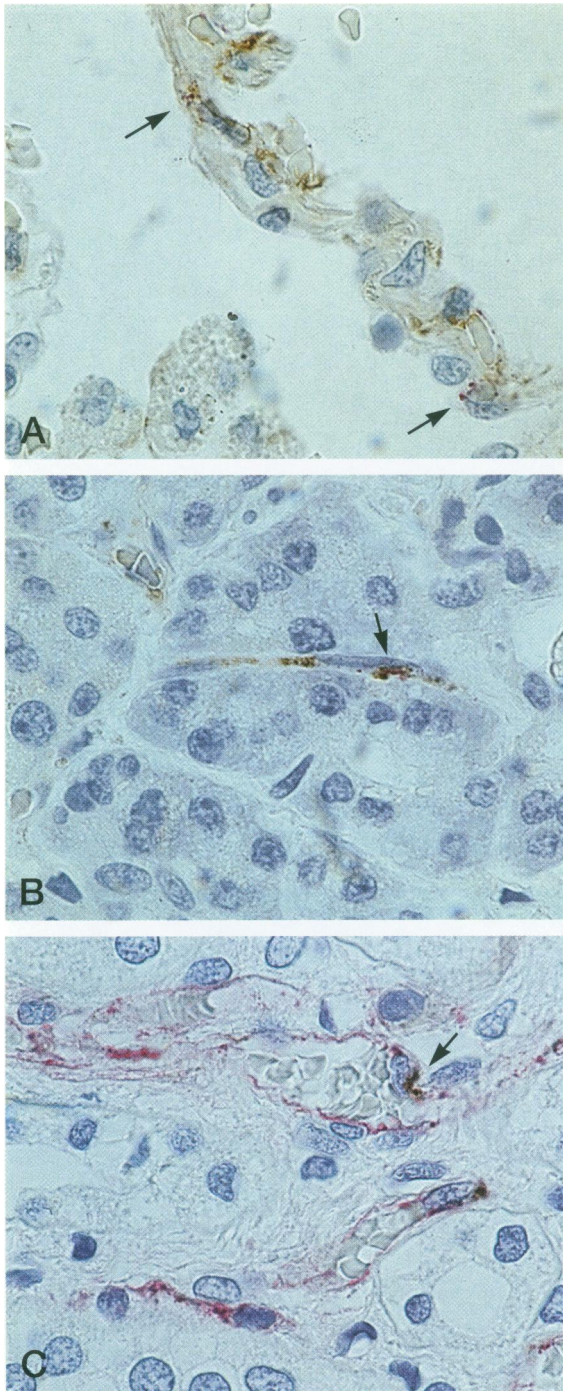
Figure 10. *Identification of SNV-infected endothelial cells by double immunostaining for SNV antigens (arrows) and endothelial markers in HPS patients. (A and B) Case 17. Immunostaining of SNV nucleocapsid proteins (alkaline phosphatase/red) and Factor VIII (peroxidase/brown) in lung (A) and pancreas (B). (C) Case 38. Double-labeling for SNV (peroxidase/brown) and endothelial marker CD31 (alkaline phosphatase/red) in kidney. Note colocalization of viral proteins and endothelial antigens. (Original magnifications: A–C, ×250).*

most closely related to PH and PUU viruses. This observation is in agreement with results of the recent phylogenetic analysis of the SNV genome.[5,19,34] The characterization of the reactivity pattern of hantaviral monoclonal and polyclonal antibodies on formalin-fixed tissues will be invaluable in expanded studies of the spectrum of hantaviral-related illnesses.

Using the large number of cases brought into this series by a broad surveillance mechanism, we were able to confirm the basic histopathological features of the syndrome[4,35] and document a wider spectrum of cases, including some with more severe histological findings. The most consistent histopathological features were observed in the lung and spleen. We consistently found large immunoblasts in the red pulp and in the periarteriolar lymphocytic sheath of spleens from HPS patients. In the lungs, the basic histopathological finding was that of an interstitial pneumonitis with variable amounts of mononuclear cell infiltration, congestion, and both interstitial and intraalveolar edema. Although the pulmonary pathological features seen in typical cases of HPS are similar to those seen in tissues of most patients who die in the exudative phase of diffuse alveolar damage (DAD),[36-40] the features are not identical. In typical HPS cases, hyaline membranes are focal, composed mainly of fibrin with little cellular debris, and reactive type II pneumocytes and neutrophils are not prominent histological features. However, these differences may reflect the fact that the earliest stages of DAD are not commonly seen as autopsy cases and that biopsies are not systematically performed in the early phases of adult respiratory distress syndrome cases. The changes observed in HPS may thus reflect the early changes of DAD, with death ensuing before the typical destructive changes associated with DAD can occur. Alternatively, the histological changes seen in HPS may represent a unique pattern of acute lung injury distinct from DAD. Of interest in this regard is the finding of more characteristic and typical histopathological features of exudative and proliferative stages of DAD in three HPS patients examined in this series. The average survival of these three patients was significantly longer than most patients dying of HPS, and hence the more destructive changes may reflect the natural progression of disease. These histological features may also be due to other complicating factors such as oxygen toxicity or secondary infection.[36,41]

Although no single pathognomonic lesion was found that would permit certain histopathological diagnosis of SNV infection, the overall pattern of histopathological lesions and hematological findings associated with HPS appears to be distinct from that of
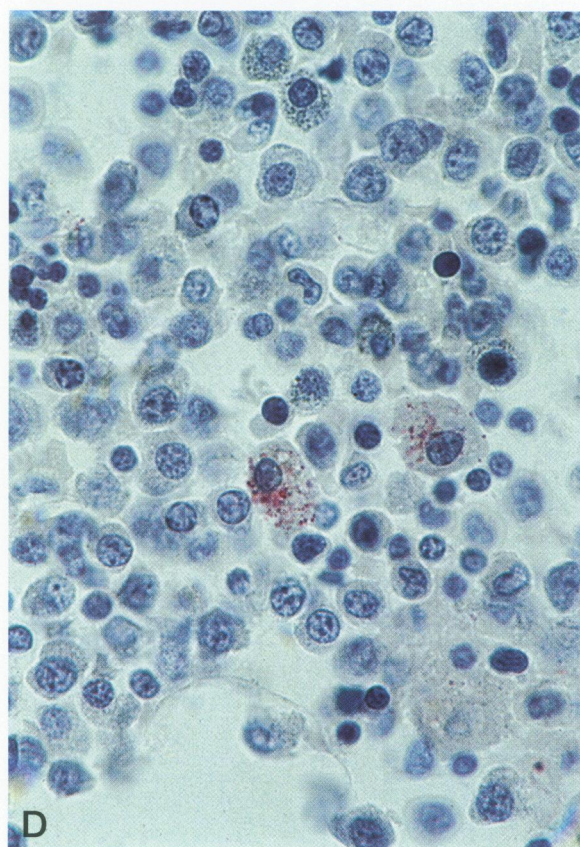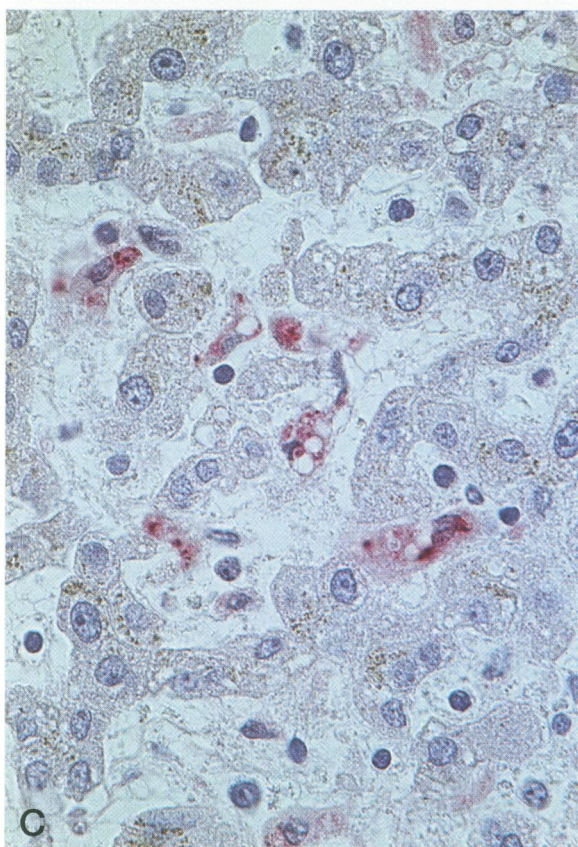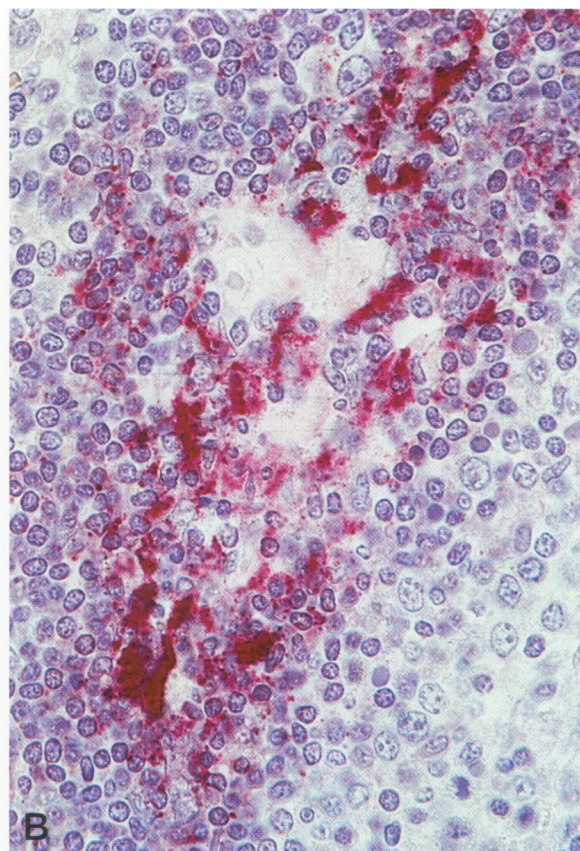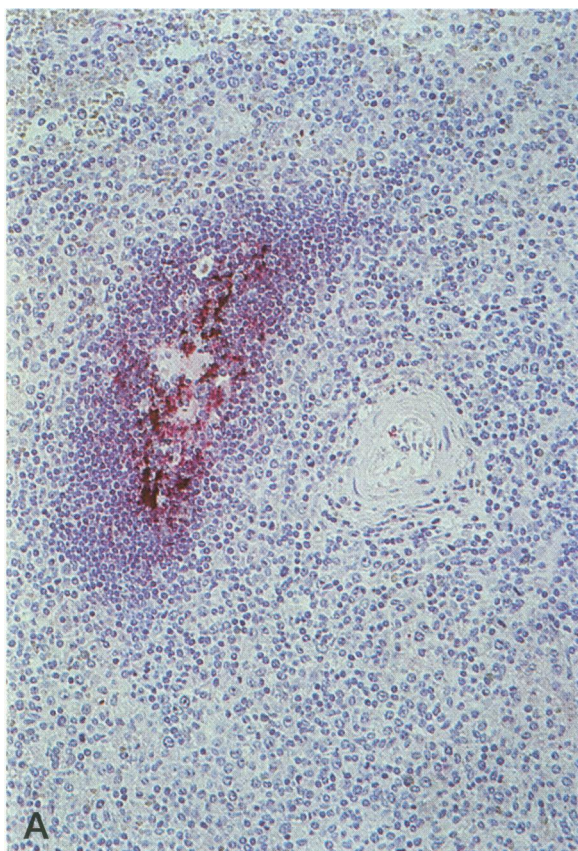
other diseases.[35] However, the differential diagnosis may be difficult, especially in the context of a wider histopathological spectrum of HPS than initially suspected, and the presence of some overlapping histological and hematological features in various infectious and noninfectious disease processes. In any event, it is clear that hematological or pathological examination is not a substitute for virus-specific diagnosis. In areas without full laboratory facilities, the hematological features of thrombocytopenia, hemoconcentration, left-shifted neutrophilic leukocytosis, and presence of atypical lymphocytes in peripheral smears may suggest the diagnosis of HPS and facilitate early disease recognition and appropriate therapy.

In this study, several lines of evidence allowed for a precise characterization of viral tropism and its consequences. Endothelial cells had a remarkably high viral load, with hantaviral antigens consistently seen in capillary endothelial cells in various tissues throughout the body. The extent of pulmonary endothelial involvement in HPS patients was remarkable, with hardly any of the cells of the lung microcirculation remaining uninfected. Despite the presence of extensive hantaviral antigens in endothelial cells, we found little evidence of endothelial cytopathic effect by light microscopy. Hantaviruses have been previously propagated in several endothelial cell lines, and antigen has been detected in vascular endothelia of patients with fatal HFRS and mice experimentally infected with HTN virus.[42-46] Thus, the tropism of SNV to endothelial cells of HPS patients may not be considered exceptional, but the extent of involvement of the pulmonary vasculature was far greater than that previously seen with other hantaviral syndromes. The magnitude and extent of pulmonary endothelial involvement in HPS would predict that the terminal shock syndrome would be most difficult to manage clinically, and this is the case in fact. Increased vascular permeability is the hallmark of the pathological events seen in HPS with hemoconcentration and pulmonary edema. These features may all stem from endothelial damage and dysfunction, as is thought to be the case with HFRS. Because pulmonary edema is an uncommon complication of HFRS, the primary target organs appear to differ in the two syndromes, with the retroperitoneal compartment including the kidneys involved primarily in HFRS and the lungs in HPS. Although large mononuclear cells with the ap-

pearance of immunoblasts are seen in both HPS and HFRS, the distribution is different. In HPS, apart from their presence in lymphoid organs, immunoblasts are primarily concentrated in the lungs of patients dying with the disease. This feature has not been reported to be a prominent finding in lungs of patients with HFRS. Our preliminary data on the nature of the lymphoid infiltrate in lung tissues of a few patients with HPS have identified the cells to be predominantly a mixture of T lymphocytes and macrophages. The proportion of T cells expressing the CD8 phenotype was increased in most patients examined. A recent two-color flow cytometric study of peripheral blood mononuclear cells in patients with HPS has shown evidence of activation in a significant proportion of T-cells.[35] Similar increases in CD8-positive cells in the early stages of HFRS have been reported.[47,48]

In our study of HPS patients, the microvasculature of kidneys showed appreciable amounts of SNV antigens in the medulla and glomeruli, despite the absence of significant light-microscopic changes in tubules and glomeruli. This observation may help explain the occurrence of proteinuria, sometimes massive, in many of the patients. We were unable to detect significant amounts of viral antigens in tubular epithelial cells. In contrast, IHC studies of HFRS patients and experimental mice infected with HTN virus have shown abundant amounts of hantaviral antigens in tubular epithelial cells.[44,45,49] This finding has led to the suggestion that acute renal failure, one of the primary clinical manifestations of HFRS, may be a result of direct viral invasion of renal tubules. The absence of significant tubular staining in HPS patients may explain why acute renal failure has not been a predominant finding in HPS patients.

Of interest is the finding of hantaviral proteins, sometimes extensive, in the microvasculature of cardiac tissues, despite little histological evidence of tissue damage. Clinical studies have suggested that myocardial dysfunction may contribute to the severe shock syndrome observed in HPS patients.[15,50] It is not clear from our study how the magnitude or extent of involvement of cardiac endothelial cells may contribute to the pathophysiology of the shock syndrome. Lesser endothelial involvement was present in many organs, but interestingly, hepatic endothelial cells were relatively spared. These observations may reflect the heterogeneous nature of the microvasculature of various organs.

Figure 11. (A) *Case 38. Localization of SNV antigens in lymphoid follicle of spleen. Note the delicate reticular pattern of staining. Rabbit anti-SNV serum.* (B) *Case 38. Higher magnification. Rabbit anti-SNV serum.* (C) *Case 38. Hyperplastic antigen-positive Kupffer cells within hepatic sinusoids. Rabbit anti-SNV serum.* (D) *Case 15. Macrophages containing SNV proteins as detected in bone marrow. GB04-BF07 mAb. (Original magnifications: A, ×50; B and C, ×158, D, ×250).*
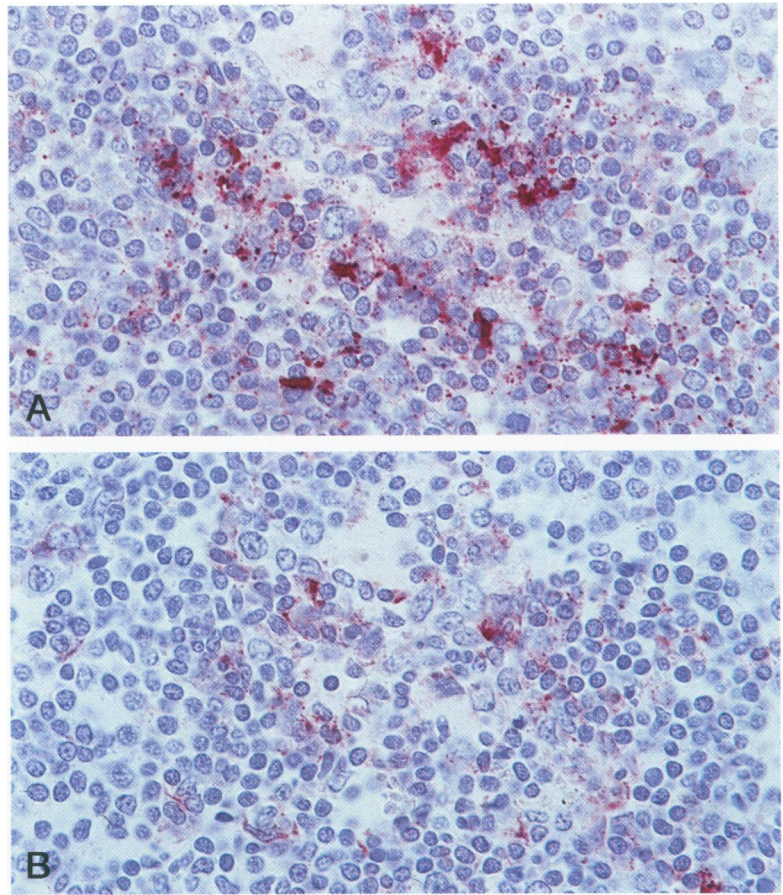
Figure 12. *Immunolabeling of a lymphoid follicle in spleen of HPS patient as seen in serial sections stained with (A) rabbit anti-SNV serum and (B) FDC1-p. Note similar labeling patterns in both sections. (Original magnifications: A and B, ×158).*

After endothelial staining, the second main immunostaining pattern seen was observed in lymphoid follicles of spleens and lymph nodes and was not distinctly associated with individual cells. Immunolabeling experiments demonstrated that this type of staining within germinal centers was associated with FDCs. These findings indicate that the network of FDCs is an important reservoir of SNV antigens. FDCs are immune accessory cells involved in the processing and presentation of antigens.[51] Antibody appears to be required to localize antigen on FDCs,[52] and the special antigen-trapping role of these cells is manifested by selected surface binding of antigen-antibody complexes. Possible events leading to a concentration of hantaviral antigens at this site include 1) trapping of antigen-antibody complexes in the expanded meshwork of cell processes (the reticular dendritic pattern of SNV localization is strikingly similar to that described for the deposition of circulating antigen-antibody complexes in experimental animals and patients infected with human immunodeficiency virus[53-58]); 2) productive viral replication in the dendritic cells themselves, initiated by some infected particles, once trapped; and 3) direct transmission of the virus from mononuclear cells to FDCs and replication within this site. Whether the FDC-associated antigens originate exclusively from extracellular trapping, or whether the virus actually replicates in FDCs, remains unknown. Other lymphoreticular cells that were observed to contain lesser amounts of hantaviral antigens included macrophages, Kupffer cells, and lymphocytes.

Detection of SNV antigens in particular cell types does not necessarily indicate viral infection or replication. Thus, we cannot exclude the possibility that the immunolocalization of hantaviral antigens might represent either phagocytosis of extracellular virions or entrapment. Our ultrastructural observations confirmed the infection of endothelial cells and macrophages in the lungs of HPS patients. The virus or virus-like particles we observed in HPS tissues were infrequent and extremely difficult to identify because of the considerable degree of pleomorphism and also the postmortem deterioration of tissues. This observation is consistent with previous reports pertaining to the morphological features of hantaviruses in tissue
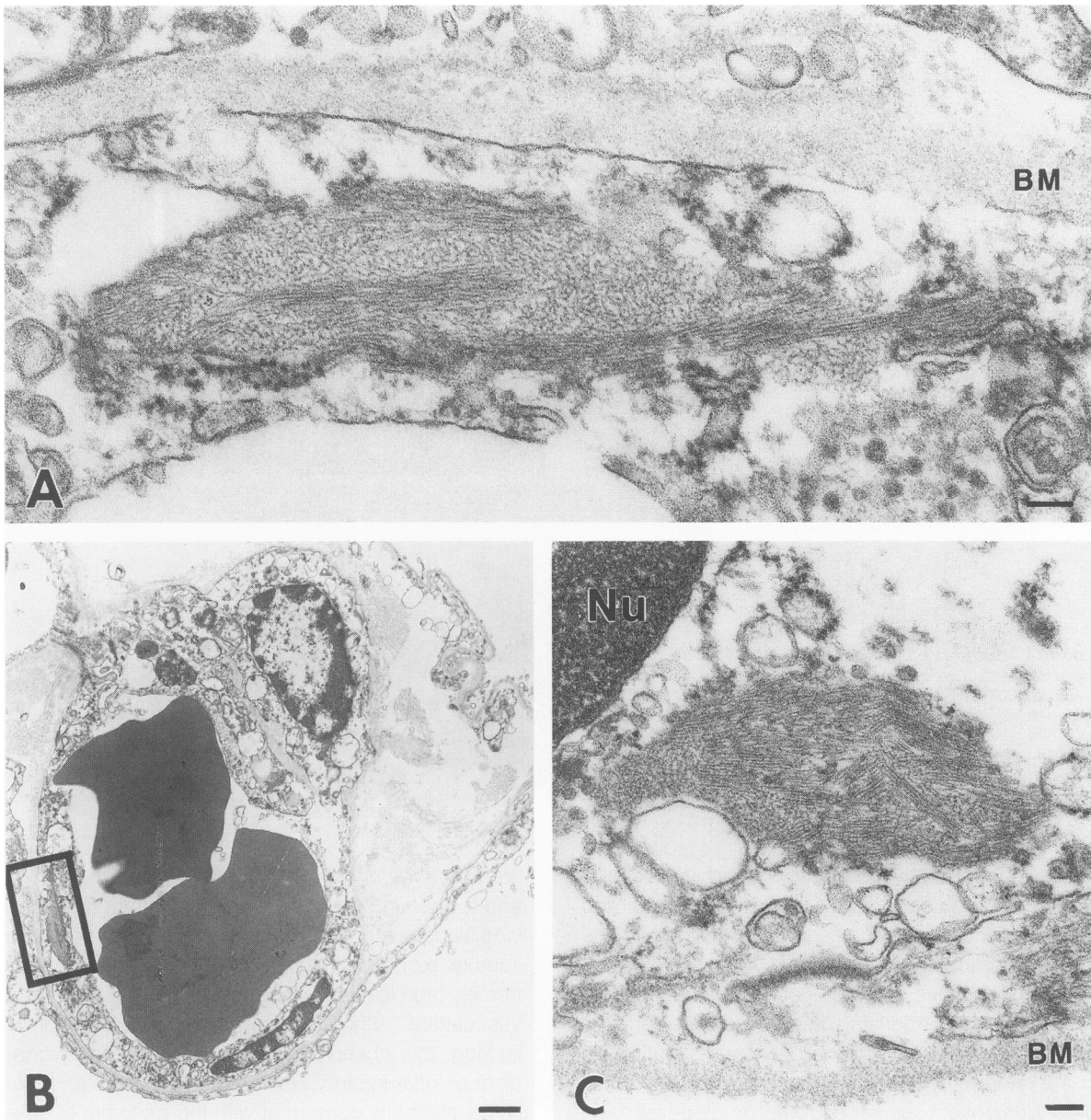
Figure 13. *Case 38. Typical hantaviral inclusions as seen within the pulmonary microvasculature.* (**A**) *High-power magnification of boxed area in* (**B**) *showing a granulofilamentous inclusion within capillary endothelium.* (**C**) *Another hantaviral inclusion seen in close proximity to an endothelial cell nucleus. Inclusions are often associated with the Golgi and/or rough endoplasmic reticulum. BM, basement membrane; NU, nucleus. (Scale bars:* **A** *and* **C**, *100 nm;* **B**, *1 μ).*

culture and autopsy tissues.[22,59,60] Despite their appearance, without definitive immunolabeling we prefer to describe these as virus-like particles. On the other hand, typical hantaviral inclusions were seen more frequently and their identity was confirmed by immunolabeling. Similar inclusions have been observed in epithelial cells of patients with HFRS and are considered to be ultrastructural markers of hantavirus-infected cells.[20] Inclusions are structures

composed of excess viral components that are synthesized by infected cells replicating the virus. Thus, our finding of inclusions in endothelial cells is consistent with viral replication in this site. Additional studies employing *in situ* hybridization are needed to examine the issue of viral replication in human tissue. Our EM findings further emphasize the lack of necrosis or overtly visible lesions that can account for the vascular leak in HPS patients. However, given the
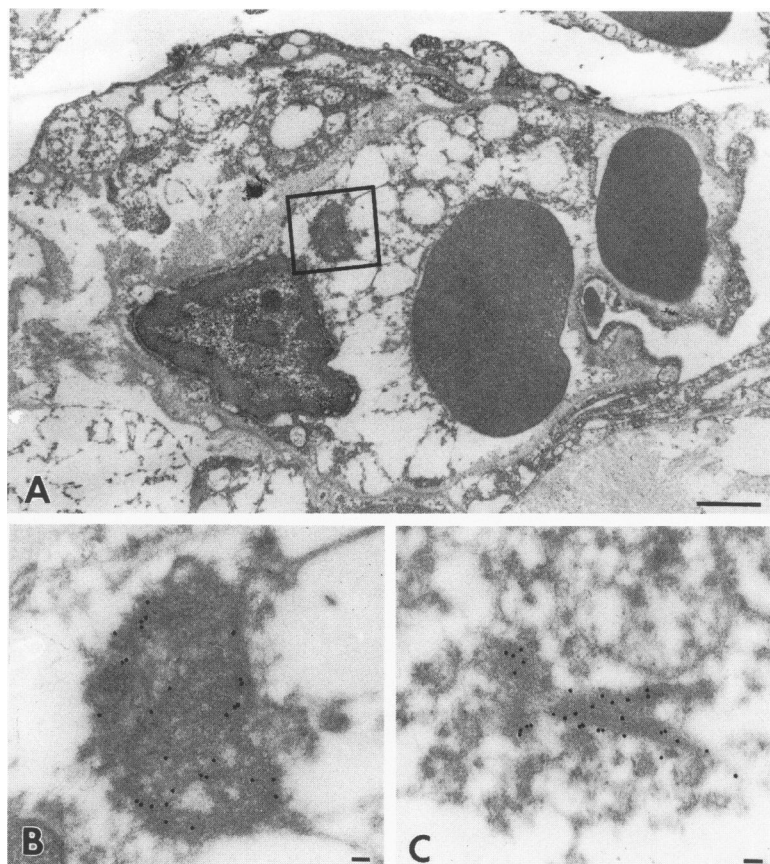
Figure 14. *Case 14. Immunogold-labeling of hantaviral inclusions seen in pulmonary endothelial cells* (A) *Low-power view showing accumulation of gold particles over a perinuclear inclusion (boxed area). (B and C) Higher power view of inclusions specifically labeled for hantavirus proteins using* Peromyscus *serum. (Scale bars: A, 1 μ; B and C, 100 nm).*

remarkable reparative capability of endothelial cells, we cannot exclude the possibility that transient and morphologically subtle changes may underlie the functional impairment. Further EM studies with optimally fixed tissues may be useful in this regard.

Whatever the underlying mechanisms, we can conclude that pulmonary edema plays an essential role in the fatal outcome of infection and that functional derangement of vascular endothelium appears to be central to the pathogenesis of HPS. However, it is unclear how the shock syndrome in this disease relates to factors such as viral distribution and immunological and pharmacological mediators of capillary permeability (Figure 16). Nevertheless, the results reported here may have important implications for understanding how these factors relate to HPS pathogenesis.

There is considerable diversity and heterogeneity of the microvasculature tissues. Endothelial cells lining the pulmonary vessels are functionally different from those of other vascular beds.[61,62] Furthermore, endothelial cells may be induced to increase the expression of constitutive molecules or express new molecules normally absent from resting microvasculature. This process, endothelial activation, is medi-

ated by a variety of chemical mediators and stimuli and is seen in different diseases.[63–68] Our data provide evidence for compartmentalization of a selective immune response in the lung in combination with extremely high levels of viral antigens in the pulmonary vasculature. Although experimental confirmation is lacking, this observation suggests that the mechanism of inflammatory cell recruitment in the lungs of HPS patients is consistent with the principle of specific attraction and adherence of a selective population of inflammatory cells to a specialized activated endothelium.[62,69,70]

This study also emphasizes the importance of macrophages, FDCs, and other cells of the mononuclear phagocytic system in the localization of hantaviral antigens and particles. Because macrophages and lymphocytes are the source of a number of active cytokines, it is possible that these infected cells may mediate localized inflammatory sequelae as well as systemic altered immunoregulatory phenomena. FDCs harbor very little or no Fc receptors, whereas they express complement receptors at high levels.[51] Therefore, the possibility that activation of the complement system may contribute to viral patho-
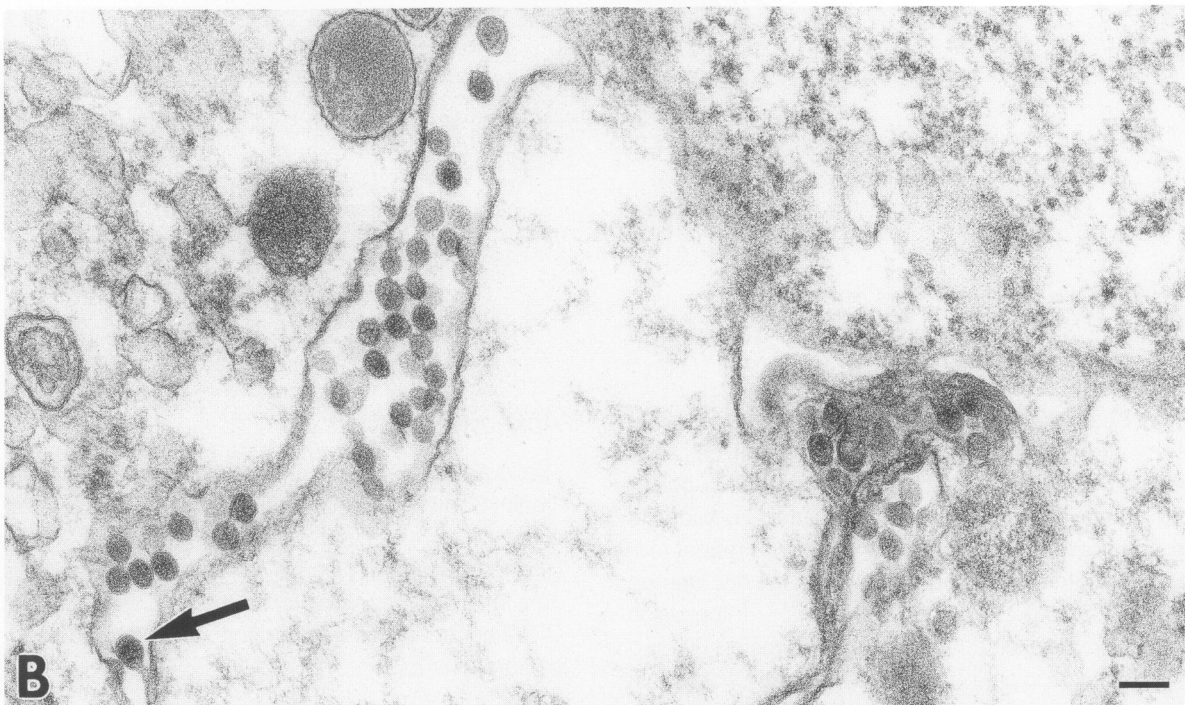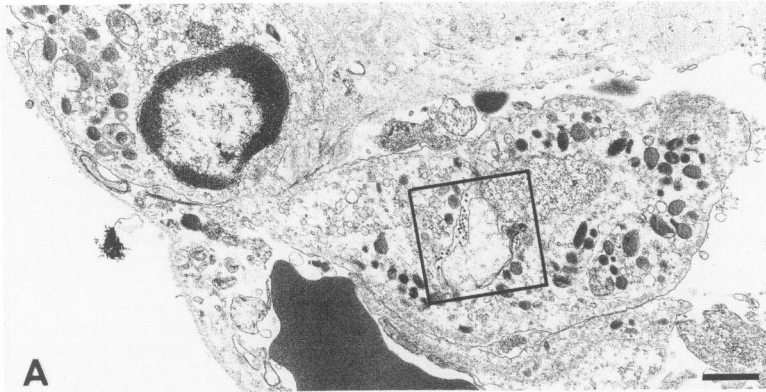
Figure 15. *Case 38. Collection of virus-like particles in a pulmonary macrophage.* (A) *Interstitial macrophage showing virus-like particles in association with a phagolysosome containing fragments of cellular debris.* (B) *Higher magnification of boxed area showing an accumulation of several virus-like particles, including one budding particle (arrow). (Scale bars: A, 1 μ; B, 100 nm).*

genesis remains to be investigated. Immune complexes have been implicated in the pathogenesis of HFRS.[71-75]

In HPS patients, there has been relatively little hemorrhage despite significant thrombocytopenia, abnormal clotting functions, and widespread endothelial infection. Thrombocytopenia, in the absence of clinical manifestations of bleeding, has also been seen in other viral hemorrhagic fevers.[76,77] The mechanism(s) of thrombocytopenia in HPS patients is unclear. However, the presence of normal or increased numbers of megakaryocytes in bone marrow, together with evidence of fibrinolysis, suggests that increased consumption or sequestration are likely causes. We found no evidence that thrombocytopenia may arise from megakaryocyte infection, as has been observed with some arenaviruses.[78] The pos-

sible presence of immune complexes in HPS patients may cause diminished platelet counts by inducing platelet aggregation, complement-mediated lysis, and sequestration by the reticuloendothelial system.

HPS is a prime example of emerging infectious diseases that continue to be recognized in the United States and elsewhere.[79,80] Interagency cooperation and epidemiological and laboratory readiness allowed for the prompt elucidation of the cause of this disease and the public health response to the outbreak of HPS in the spring of 1993.[81] Although the initial cases of HPS were recognized in the Four Corners area, additional cases continue to be identified in other regions of the United States and Canada.[82-84] Evidence for different hantaviral genetic strains and the spectrum of associated illnesses in North America continues to evolve.[19,85] Several species of rodents
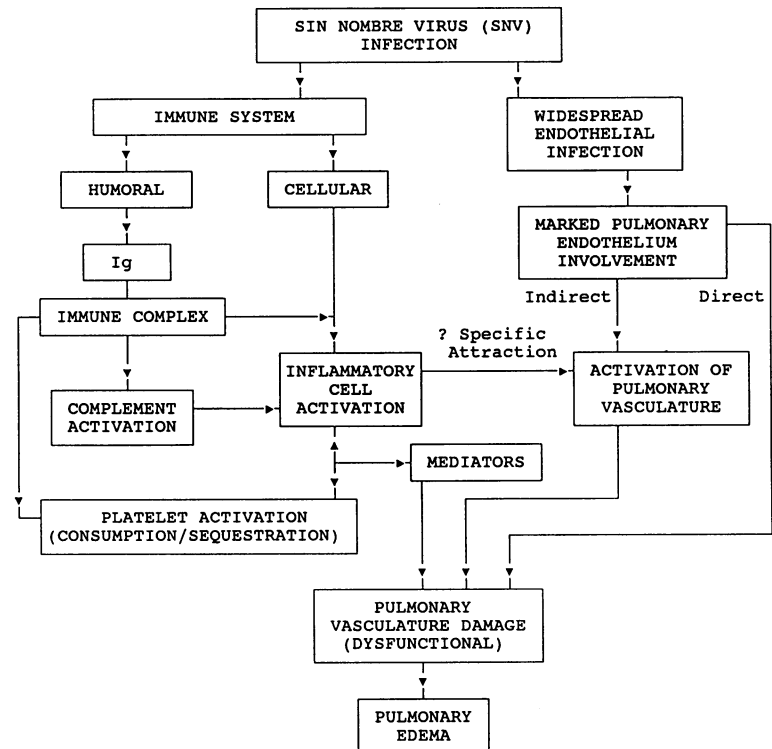
Figure 16. *Flow diagram of possible mechanisms of pulmonary edema in patients with HPS.*

have been identified as reservoirs for hantaviruses in the United States.[7,86] Retrospective fatal cases of HPS have been identified as early as 1983, suggesting that recent environmental and ecological changes are primarily responsible for the recent recognition of this new hantavirus and for the occurrence of the HPS outbreak in the Southwest.[4,87] Information regarding the clinicopathological features of HPS and the cellular tropism of SNV and its distribution within human tissues is important for understanding the pathogenesis of HPS. It is hoped that detailed knowledge of the mechanisms involved in the process of accumulation of the inflammatory cells and in the development of the severe pulmonary edema may lead to specific forms of therapeutic intervention in HPS patients.

Note Added in Proof

Hantaviruses are typically named after a distinctive geographic feature or the locale where that virus was first recognized. Several names were initially considered for the newly isolated virus from the recent HPS outbreak in the southwestern United States. Names including "Four Corners virus" and "Muerto Canyon virus" have been used in previous reports. Because of objections and concerns from local residents, the name was changed to "Sin Nombre virus" ("virus without a name") after consultation between CDC investigators and representatives from the local community.

Acknowledgments

References

1. Centers for Disease Control and Prevention: Outbreak of acute illness–southwestern United States, 1993. Morb Mortal Wkly Rep 1993, 42:421–424
2. Centers for Disease Control and Prevention: Update: outbreak of hantavirus infection–southwestern United States, 1993. Morb Mortal Wkly Rep 1993, 42:441–443
3. Centers for Disease Control and Prevention: Update: outbreak of hantavirus infection–southwestern United States, 1993. Morb Mortal Wkly Rep 1993, 42:477–479
4. Centers for Disease Control and Prevention: Update: hantavirus pulmonary syndrome–United States, 1993. Morb Mortal Wkly Rep 1993, 42:816–820
5. Nichol ST, Spiropoulou CF, Morzunov S, Rollin PE, Ksiazek TG, Feldmann H, Sanchez A, Childs J, Zaki S, Peters CJ: Genetic identification of a hantavirus associated with an outbreak of acute respiratory illness. Science 1993, 262:914–917

6. Zaki SR, Greer PW, Coffield LM, Nolte KB, Zumwalt R, Umland ET, Feddersen RM, Foucar K, Ruo SL, Rollin P, Ksiazek T, Nichol S, Peters CJ: Outbreak of hantavirus-associated illness in the United States: immunohistochemical localization of viral nucleoproteins to endothelial cells in human tissues. Lab Invest 1994, 70:129A (Abstr.)

7. Childs J, Ksiazek T, Spiropoulou C, Krebs J, Morzunov S, Maupin G, Gage K, Rollin P, Sarisky J, Enscore R, Frey J, Peters CJ, Nichol S: Serologic and genetic identification of Peromyscus maniculatus as the primary rodent reservoir for a new hantavirus in the southwestern United States. J Infect Dis 1994, 169: 1271–1280

8. Elliott LH, Ksiazek TG, Rollin PE, Spiropoulou CF, Morzunov S, Monroe M, Goldsmith CS, Humphrey CD, Zaki SR, Krebs JW, Maupin G, Gage K, Childs JE, Nichol ST, Peters CJ: Isolation of the causative agent of hantavirus pulmonary syndrome. Am J Trop Med Hyg 1994, 51:102–108

9. Schmaljohn CS: Nucleotide sequence of the L genome segment of Hantaan virus. Nucleic Acids Res 1990, 18:6728

10. Schmaljohn CS, Dalrymple JM: Analysis of Hantaan virus RNA: evidence for a new genus of Bunyaviridae. Virology 1983, 131:482–491

11. Xiao SY, Leduc JW, Chu YK, Schmaljohn CS: Phylogenetic analyses of virus isolates in the genus Hantavirus, family Bunyaviridae. Virology 1994, 198:205–217

12. Chu YK, Rossi C, Leduc JW, Lee HW, Schmaljohn CS, Dalrymple JM: Serological relationships among viruses in the Hantavirus genus, family Bunyaviridae. Virology 1994, 198:196–204

13. Leduc JW: Epidemiology of Hantaan and related viruses. Lab Anim Sci 1987, 37:413–418

14. Lee HW: World Health Organization (WHO) Collaborating Center for Virus Reference and Research. In Manual of Hemorrhagic Fever with Renal Syndrome. Edited by HW Lee and JM Dalrymple. Korea University, Seoul, South Korea, 1989, pp 11–18

15. Duchin J, Koster F, Peters CJ, Simpson G, Tempest B, Zaki S, Ksiazek T, Rollin P, Nichol S, Umland E, Moolenaar R, Reef S, Nolte K, Gallagher M, Butler J, Breiman R, Hantavirus Study Group: Hantavirus pulmonary syndrome: a clinical description of 17 patients with a newly recognized disease. N Engl J Med 1994, 330:949–955

16. Ruo SL, Sanchez A, Elliott LH, Brammer LS, McCormick JB, Fisher-Hoch SP: Monoclonal antibodies to three strains of hantaviruses: Hantaan, R22, Puumala. Arch Virol 1991, 119:1–11

17. Ksiazek TG, Peters CJ, Rollin PE, Zaki SR, Nichol S, Spiropoulou CF, Morzunov S, Feldman H, Sanchez A, Khan A, Mahy B, Wachsmuth K, Butler J: Identification of a new North American hantavirus that causes acute pulmonary insufficiency. Am J Trop Med Hyg 1995, 52:1017–1023

18. Feldmann H, Sanchez A, Morzunov S, Spiropoulou CF,

Rollin PE, Ksiazek TG, Peters CJ, Nichol ST: Utilization of autopsy RNA for the synthesis of the nucleocapsid antigen of a newly recognized virus associated with hantavirus pulmonary syndrome. Virus Res 1993, 30: 351–367

19. Spiropoulou CF, Morzunov S, Feldmann H, Sanchez A, Peters CJ, Nichol ST: Genome structure and variability of a virus causing hantavirus pulmonary syndrome. Virology 1994, 200:715–723

20. Hung T, Xia S, Chou Z, Gan S, Yanagihara R: Morphology and morphogenesis of viruses of hemorrhagic fever with renal syndrome: inclusion bodies–ultrastructural marker of hantavirus-infected cells. Intervirology 1987, 27:45–52

21. Goldsmith CS, Humphrey CD, Elliott LH, Zaki SR: Morphology of Muerto Canyon virus, causative agent of hantavirus pulmonary syndrome. Proceedings of the Fifty-Second Annual Meeting of the Microscopy Society of America 1994, 1:272–273

22. Hung T, Chou Z, Zhao T, Xia S, Hang C: Morphology and morphogenesis of viruses of hemorrhagic fever with renal syndrome (HFRS): some peculiar aspects of the morphogenesis of various strains of HFRS virus. Intervirology 1985, 23:97–108

23. LeDuc J, Ksiazek T, Rossi C, Dalrymple J: A retrospective analysis of sera collected by the hemorrhagic fever commission during the Korean conflict. J Infect Dis 1990, 162:1182–1184

24. Lukes R: The pathology of thirty-nine fatal cases of epidemic hemorrhagic fever. Am J Med 1954, 16:639–650

25. Steer A: Pathology of hemorrhagic fever: a comparison of the findings–1951 and 1952. Am J Pathol 1955, 31:201–221

26. Swift W Jr.: Clinical aspects of the renal phase of epidemic hemorrhagic fever. Ann Intern Med 1953, 38: 102–105

27. Kim D: Clinical analysis of 111 fatal cases of epidemic hemorrhagic fever. Am J Med 1965, 39:218–220

28. Linderholm M, Billstrom A, Settergren B, Tarnvik A: Pulmonary involvement in nephropathia epidemica as demonstrated by computed tomography. Infection 1992, 20:263–266

29. Lahdevirta J: The minor problem of hemostatic impairment in nephropathia epidemica, the mild Scandinavian form of hemorrhagic fever with renal syndrome. Rev Infect Dis 1989, 11(S4):S860–S863

30. Lahdevirta J: Clinical features of HFRS in Scandinavia as compared with East Asia. Scan J Infect Dis 1982, S36:93–95

31. Lee M, Kim B, Kim S, Park S, Han J, Kim S, Lee J: Coagulopathy in hemorrhagic fever with renal syndrome (Korean hemorrhagic fever). Rev Infect Dis 1989, 11-(S4):S877–S883

32. Entwisle G, Hale E: Hemodynamic alterations in hemorrhagic fever. Circulation 1957, 15:414–425

33. Powell GM: Hemorrhagic fever: a study of 300 cases. Medicine 1954, 33:97–153

34. Hjelle B, Jenison S, Torrez-Martinez N, Yamada T, Nolte K, Zumwalt R, Myers G: A novel hantavirus associated with an outbreak of fatal respiratory disease in the southwestern United States: evolutionary relationships to known hantaviruses. J Virol 1994, 68:592–596

35. Nolte KB, Feddersen RM, Foucar K, Zaki SR, Koster FT, Madar D, Merlin TL, McFeeley PJ, Umland ET, Zumwalt RE: Hantavirus pulmonary syndrome in the United States: pathologic description of a disease caused by a new agent. Hum Pathol 1995, 26:110–120

36. Katzenstein A, Bloor C, Leibow A: Diffuse alveolar damage–the role of oxygen, shock, and related factors. Am J Pathol 1976, 85:210–224

37. Pratt P: Pathology of adult respiratory distress syndrome: implications regarding therapy. Semin Res Med 1982, 4:79–85

38. Simon R, Ward P: Adult respiratory distress syndrome. Inflammation: Basic Principles and Clinical Correlates. Edited by JI Gallin, IM Goldstein, and R Snyderman. New York, Raven Press, Ltd., 1992, pp 999–1016

39. Hill JD, Ratliff J, Parrott JW, Lamy M, Fallat R, Koeniger E, Yaeger E, Whitmer G: Pulmonary pathology in acute respiratory insufficiency: lung biopsy as a diagnostic tool. J Thorac Cardiovasc Surg 1976, 71:64–71

40. Katzenstein A, Askin F: Acute lung injury patterns: Diffuse alveolar damage, acute interstitial pneumonia, bronchiolitis obliterans–organizing pneumonia. Surgical Pathology of Non-Neoplastic Lung Disease. Edited by J Bennington. Philadelphia, W.B. Saunders Company, 1990, pp 9–57

41. Nash G, Blennerhassett JB, Pontoppidan H: Pulmonary lesions associated with oxygen therapy and artificial ventilation. N Engl J Med 1967, 276:368–374

42. Yanagihara R, Silverman DJ: Experimental infection of human vascular endothelial cells by pathogenic and nonpathogenic hantaviruses. Arch Virol 1990, 111:281–286

43. Pensiero M, Sharefkin J, Dieffenbach C, Hay J: Hantaan virus infection of human endothelial cells. J Virol 1992, 66:5929–5936

44. Kurata T, Tsai T, Bauer S, McCormick J: Immunofluorescence studies of disseminated Hantaan virus infection of suckling mice. Infect Immun 1983, 41:391–398

45. Kurata T, Sata T, Aoyama Y, Yamamishi K, Domae K, Yamanouchi T, Tsai T, Wear D: Systemic deposition of viral antigens in the vascular endothelia of hemorrhagic fever with renal syndrome. Cellular, Molecular and Genetic Approaches to Immunodiagnosis and Immunotherapy. Edited by K Kano, S Mori, T Sugisaki, M Torisu. Tokyo, University of Tokyo Press, 1987, pp 305–312

46. Zhu P, Yang W: Effects of Hantaan virus on human endothelial cells and their significance in pathogenesis of hemorrhagic fever with renal syndrome. Chin Med J 1991, 104:924–929

47. Chen L, Yang W: Abnormalities of T cell immunoregulation in hemorrhagic fever with renal syndrome. J Infect Dis 1990, 161:1016–1019

48. Tang Y, Yang W, Zhang W, Bai X: Localization and changes of hemorrhagic fever with renal syndrome virus in lymphocyte subpopulation. Chin Med J 1991, 104:673–678

49. Kim S, Kang E, Kim Y, Han J, Lee J, Kim Y, Hall WC, Dalavmple JM, Peters CJ: Localization of Hantaan viral envelope glycoproteins by monoclonal antibodies in renal tissues from patients with Korean hemorrhagic fever. Am J Clin Pathol 1993, 100:398–403

50. Levy H, Simpson SQ: Hantavirus pulmonary syndrome. Am J Respir Crit Care Med 1994, 149:1710–1713

51. Schriever F, Nadler L: The central role of follicular dendritic cells in lymphoid tissue. Adv Immunol 1992, 51:243–284

52. MacLennan IM: Germinal centers. Annu Rev Immunol 1994, 12:117–139

53. Chakrabarti L, Isola P, Cumont M, Claessens-Maire M, Hurtrel M, Montagnier L, Hurtrel B: Early stages of simian immunodeficiency virus infection in lymph nodes. Am J Pathol 1994, 144:1226–1237

54. Parmentier H, van Wichen D, Sie-Go DDS, Goudsmit J, Borleffs JC, Schuurman H: HIV-1 infection and virus production in follicular dendritic cells in lymph nodes: a case report, with analysis of isolated follicular dendritic cells. Am J Pathol 1990, 137:247–251

55. Spiegel H, Herbst H, Niedobitek G, Foss H, Stein H: Follicular dendritic cells are a major reservoir for human immunodeficiency virus type 1 in lymphoid tissues facilitating infection of CD4 T-helper cells. Am J Pathol 1992, 140:15–22

56. Tenner-Racz K, Racz P, Bofill M, Schulz-Meyer A, Dietrich M, Kern P, Weber J, Pinching AJ, Veronese-Dimarzo F, Popovic M, Klatzmann D, Gluckman JC, Janossy G: HTLV-III/LAV viral antigens in lymph nodes of homosexual men with persistant lymphodenopathy and AIDS. Am J Pathol 1986, 123:9–15

57. Schuurman H, Krone WA, Broekhuizen R, Goudsmit J: Expression of RNA and antigens of human immunodeficiency virus type-1 (HIV-1) in lymph nodes from HIV-1 infected individuals. Am J Pathol 1988, 133:516–524

58. Ringler DJ, Wyand MS, Walsh DG, MacKey JJ, Chalifoux LV, Popovic M, Minassian AA, Sehgal PK, Daniel MD, Desrosiers RC, King NW: Cellular localization of simian immunodeficiency virus in lymphoid tissues. I. Immunochemistry and electron microscopy. Am J Pathol 1989, 134:373–383

59. Hung T, Zhou JY, Tang YM, Zhao TX, Baek LJ, Lee HW: Identification of Hantaan virus-related structures in kidneys of cadavers with haemorrhagic fever with renal syndrome. Arch Virol 1992, 122:187–199

60. Kikuchi K, Imamura M, Ueno H, Takami T, Koshiba H,

Ogawa K, Dempo K, Mori M, Minase T, Yoshida Y, Muroya K: An autopsy case of epidemic hemorrhagic fever (Korean hemorrhagic fever). Sapporo Medical Journal 1982, 51:K17–K31

61. Belloni PN, Carney DH, Nicolson GL: Organ-derived microvessel endothelial cells exhibit differential responsiveness to thrombin and other growth factors. Microvasc Res 1992, 43:20–45

62. Pilewski J, Albelda S: Adhesion molecules in the lung. Am Rev Respir Dis 1993, 148:S31–S37

63. Pober J: Cytokine-mediated activation of vascular endothelium–Physiology and pathology. Am J Pathol 1988, 133:426–433

64. Huynh H, Dorovini-Zis K: Effects of gammainterferon on primary cultures of human brain microvessel endothelial cells. Am J Pathol 1993, 142:1265–1278

65. Mantovani A, Bussolino F, Dejana E: Cytokine regulation of endothelial cell function. FASEB 1992, 6:2591–2599

66. Brown Z, Gerritsen M, Carley W, Strieter R, Kunkel S, Westwick J: Chemokine gene expression and secretion by cytokine-activated human microvascular endothelial cells. Am J Pathol 1994, 145:913–921

67. Munro JM, Pober J, Cotran R: Tumor necrosis factor and gamma interferon induce distinct patterns of endothelial activation and associated leukocyte accumulation in skin of Papio anubis. Am J Pathol 1989, 135:121–133

68. Bevilacqua M, Nelson R, Mannori G, Ceccone O: Endothelial-leukocyte adhesion molecules in human disease. Annu Rev Med 1994, 45:361–378

69. Berman J, Beer D, Theodore A, Kornfeld H, Bernardo J, Center D: Lymphocyte recruitment to the lung. Am Rev Respir Dis 1990, 142:238–257

70. Jones M, Hoover R, Meyrick B: Endotoxin enhancement of lymphocyte adherence to cultured sheep lung microvascular endothelial cells. Am J Respir Cell Mol Biol 1992, 7:81–89

71. Wang J, Yang P, Wu Q, Sun T, Xu Z, Dai Z: The role of tissue immune complex, complement activation and its immunopathologic injury in the pathogenesis of the epidemic hemorrhagic fever. Chin Med J 1984, 99:21–26

72. Cosgriff TM: Mechanisms of disease in hantavirus infection: pathophysiology of hemorrhagic fever with renal syndrome. Rev Infect Dis 1991, 13:97–107

73. Yan D, Gu X, Wang D, Yang S: Studies on immunopathogenesis in epidemic hemorrhagic fever: sequential observations on activation of the first complement component in sera from patients with epidemic hemorrhagic fever. J Immunol 1981, 127:1064–1067

74. Gu X, Wang D, Yang S, Yan D: Activation of the alternative complement pathway in patients with epidemic hemorrhagic fever. Chin Med J 1984, 97:283–290

75. Lee M: Coagulopathy in patients with hemorrhagic fever with renal syndrome. J Kor Med Sci 1987, 2:201–211

76. Walker D: The pathogenesis and pathology of the hemorrhagic state in viral and rickettsial infections. CRC Handbook of Viral and Rickettsial Hemorrhagic Fevers. Edited by JS Gear. Boca Raton, Florida, CRC Press, Inc., 1988, pp 9–41

77. Mendelow B: Viral and rickettsial hemorrhagic fevers: laboratory investigation of the hemorrhagic state. CRC Handbook of Viral and Rickettsial Hemorrhagic Fevers. Edited by JS Gear. Boca Raton, Florida, CRC Press, Inc., 1988, pp 47–60

78. Murphy F, Winn W, Walker D, Flemister M, Whitfield S: Early lymphoreticular viral tropism and antigen persistence: Tamiami virus infection in the cotton rat. Lab Invest 1976, 34:125–140

79. Institute of Medicine: Emerging Infections: Microbial Threats to Health in the United States. Washington, D.C., National Academy Press, 1992

80. Centers for Disease Control and Prevention: Addressing emerging infectious disease threats. A prevention strategy for the United States. Atlanta, National Center for Infectious Diseases, Centers for Disease Control and Prevention, 1994, pp 1–46

81. Hughes JM, Peters CJ, Cohen ML, Mahy BWJ: Hantavirus pulmonary syndrome: an emerging infectious disease. Science 1993, 262:850–851

82. Centers for Disease Control and Prevention: Newly identified hantavirus–Florida, 1994. Morb Mortal Wkly Rep 1994, 43:99–105

83. Centers for Disease Control and Prevention: Hantavirus pulmonary syndrome–northeastern United States. Morb Mortal Wkly Rep 1994, 43:548–9, 555–6

84. Chapman L, Khabbaz R: Etiology and epidemiology of the Four Corners hantavirus outbreak. Infect Agents Dis 1994, 3:234–244

85. Hjelle B, Chavez-Giles F, Torrez-Martinez N, Yates T, Sarisky J, Webb J, Ascher M: Genetic identification of a novel hantavirus of the harvest mouse Reithrodontomys megalotis. J Virol 1994, 68:6751–6754

86. Rollin PE, Ksiazek TG, Elliott LH, Ravkov E, Livingstone W, Monroe M, Glass G, Ruo S, Gaines M, Khan AS, Childs JE, Nichol ST, Peters CJ: Isolation of Black Creek Canal virus, a new hantavirus from Sigmodon hispidus in Florida. J Med Virol 1995 (In press)

87. Zaki SR, Albers RC, Greer PW, Coffield LM, Armstrong LR, Khan AS, Khabbaz R, Peters CJ: Retrospective diagnosis of a 1983 case of fatal hantavirus pulmonary syndrome. Lancet 1994, 343:1037–1038

88. Tabrizchi H, Hansmann M-L, Parwaresch MR, Lennert K: Distribution pattern of follicular dendritic cells in low grade B-cell lymphomas of the gastrointestinal tract immunostained by Ki-FDC1p: a new paraffin-resistant monoclonal antibody. Mod Pathol 1990, 3:470–478

89. Radzun HJ, Hansmann M-L, Heidebrecht HJ, Bodewadt-Radzun S, Wacker HH, Kreipe H, Lumbeck H, Hernandez C, Kuhn C, Parwaresch MR: Detection of a monocyte/macrophage differentiation antigen in routinely processed paraffin-embedded tissues by monoclonal antibody Ki-M1P. Lab Invest 1991, 65:306–315